UNIVERSITAS INDONESIA

Micromagnetic Study Magnetic Domain Wall Dynamics on Permalloy Nanowires (Ni$_{80}$Fe$_{20}$)

ANDY SUMARTA
0606068032

FAKULTAS MATEMATIKA DAN ILMU PENGETAHUAN ALAM
PROGRAM STUDI FISIKA
DEPOK
Juni 2011

UNIVERSITAS INDONESIA

Micromagnetic Study Magnetic Domain Wall Dynamics on Permalloy Nanowires ($Ni_{80}Fe_{20}$)

Skripsi

Diajukan sebagai salah satu syarat untuk memperoleh gelar Sarjana Sains

ANDY SUMARTA
0606068032

FAKULTAS MATEMATIKA DAN ILMU PENGETAHUAN ALAM
PROGRAM STUDI FISIKA
DEPOK
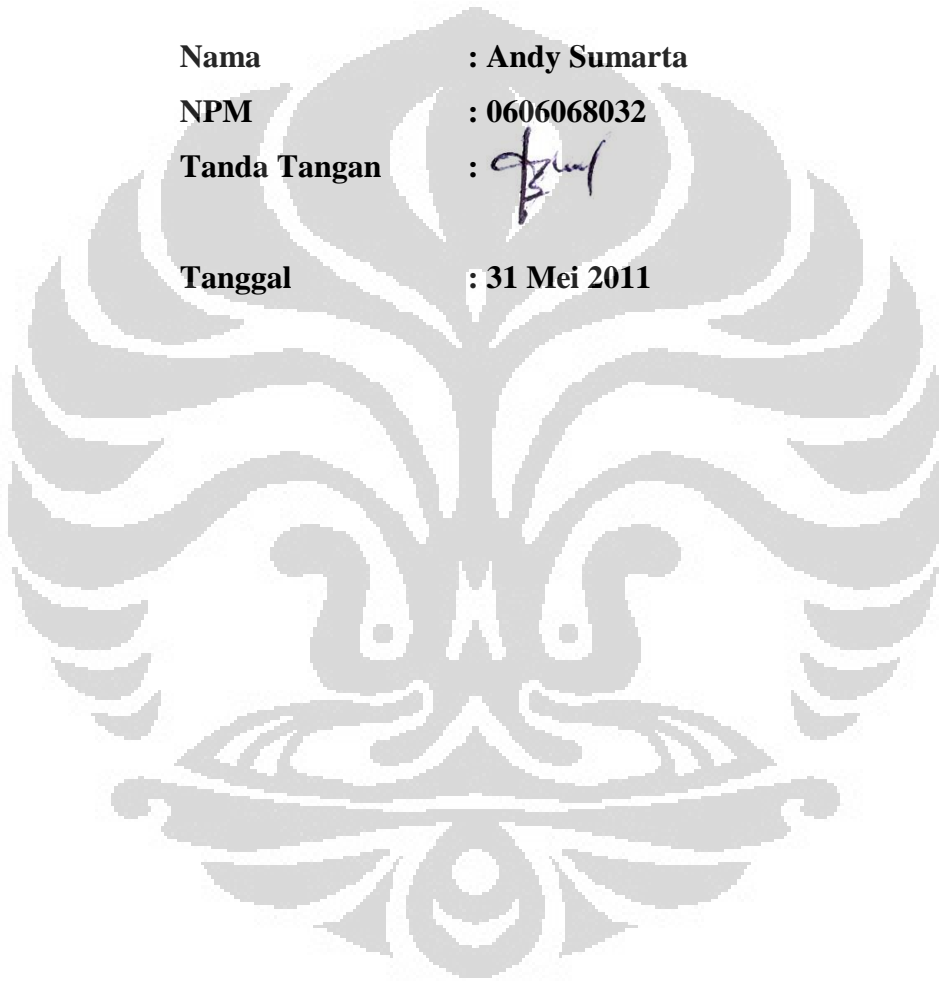**Juni 2011**

i

HALAMAN PERNYATAAN ORISINALITAS

Tugas Akhir ini adalah hasil karya saya sendiri,
dan semua sumber baik yang dikutip maupun dirujuk
telah saya nyatakan dengan benar.

Nama   **: Andy Sumarta**
NPM   **: 0606068032**
Tanda Tangan   **:**

Tanggal   **: 31 Mei 2011**
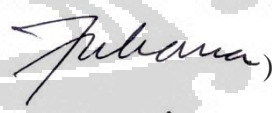
HALAMAN PENGESAHAN

Skripsi ini diajukan oleh :

Nama : Andy Sumarta

NPM : 0606068032

Program Studi : Fisika

Judul : Micromagnetic Study Magnetic Domain Wall Dynamics on Permalloy Nanowires ($Ni_{80}Fe_{20}$)

Telah berhasil dipertahankan di hadapan Dewan Penguji dan diterima sebagai bagian persyaratan yang diperlukan untuk memperoleh gelar Sarjana Sains pada Program Studi Fisika, Fakultas Matematika dan Ilmu Pengetahuan Alam, Universitas Indonesia

DEWAN PENGUJI

Pembimbing : Dr. Budhy Kurniawan ( )

Pembimbing : Dr. Dede Djuhana ( )

Penguji : Dr. Muhammad Hikam ( )

Penguji : Dr. Aziz Majidi ( )

Ditetapkan di : Depok

Tanggal : 31 Mei 2011

HALAMAN PERNYATAAN PERSETUJUAN PUBLIKASI TUGAS AKHIR UNTUK KEPENTINGAN AKADEMIS

Sebagai civitas akademik Universitas Indonesia, saya yang bertanda tangan dibawah ini:

Nama   : Andy Sumarta

NPM   : 0606068032

Program Studi : S1 Fisika

Fakultas   : Matematika dan Ilmu Pengetahuan Alam

Jenis Karya   : Skripsi

demi pengembangan ilmu pengetahuan, menyetujui untuk memberikan kepada Universitas Indonesia **Hak Bebas Royalti Noneksklusif** (*Non – exclusive Royalty - Free Right*) atas karya ilmiah saya yang berjudul:

MICROMAGNETIC STUDY MAGNETIC DOMAIN WALL DYNAMICS ON PERMALLOY NANOWIRES ($Ni_{80}Fe_{20}$)

beserta perangkat yang ada (jika diperlukan). Dengan Hak Bebas Royalti Non-eksklusif ini Universitas Indonesia berhak menyimpan, mengalih media/ for-matkan, mengelola dalam bentuk pangkalan data (data base), merawat, dan mempublikasikan tugas akhir saya selama tetap mencantumkan nama saya se-bagai penulis/ pencipta dan sebagai pemilik Hak Cipta.

Demikian pernyataan ini saya buat dengan sebenarnya.

Dibuat di : Depok

Pada tanggal : Juni 2011

Yang menyatakan

(Andy Sumarta)

iv

PREFACE

Praises and thanks to Jesus Christ for all His grace in my life, I have finished this thesis. In this chance also I want to say thanks you very much for every people who given their hand to help me in the process of writing, they are:

1. Dr. Santoso Sukirno as the head of Dept. of Physics, University of Indonesia who give a chance for me to finished my study in Dept. of Physics, University of Indonesia.

2. Prof. Dr. Rosari Saleh as the head of Condensed Matter, Dept of Physics, University of Indonesia who give a meaningful education in my life.

3. Dr. Budhy Kurniawan dan Dr. Dede Djuhana as the supervisors who teach me and guiding me to finished this thesis.

4. Dr. Muhamad Hikam dan Dr. Aziz Majidi as the examiners who willing to make a discuss and give many idea for this thesis.

5. My father, my Mother and also my aunt Afie ie who give a suport spirit for me.

6. The 38 community: Alvin, Edvan, Arkies, Hendry, Umbu, Anthony, James, Epin thanks for the togetherness, pray, and suports from you all.

7. Kak Ryky, Franky, Erni, Lidya, Tika, Gracely, Dina, bidang 1 and bidang 3 and other friends in Persekutuan Oikumene.

8. 103A community, iyan, Atul, Anni, Arnold, Sharil, Asrikin, and all friends in physics 2006.

9. Ibu Ani, ibu Elis, ibu Agnes and also colleague in SMA Mardiyuana Depok.

10. Everyone that i can't mention in this preface who give the strength, suport and guidance during arrangement of this thesis.

I hope this thesis can give a benefit for the science advancement.

Depok, Juni 2011

Penulis

v

ABSTRAK

Nama   : Andy Sumarta

Judul   : Studi Mikromagnetik pada Bahan Permalloy ($Ni_{80}Fe_{20}$)

                       Berbentuk Nanowire

Telah dilakukan pengamatan mengenai dinamika domain wall pada bahan Permalloy berbentuk nanowire dengan menggunakan software simulasi mikromagnetik OOMMF berdasarkan persamaan Landau-Lifshitz-Gilbert (LLG). Pengamatan dinamika domain wall dilakukan pada nanowire dengan panjang 2000 nm, variasi lebar dari 100 sampai 200, dan variasi ketebalan 2,5 nm dan 5,0 nm dibawah pengaruh medan magnet luar dalam bentuk pulsa. Kecepatan domain wall bertambah ketika medan magnet luar yang diberikan di perbesar dan kemudian mengalami penurunan scara drastis setelah medan magnet luar yang diberikan melampaui medan magnet kritis yang di sebut medan Walker breakdown. Sebelum medan magnet luar yang diberikan melebihi nilai medan Walker breakdown, domain wall bergerak dengan mempertahankan struktur transverse. Setelah melampaui nilai medan Walker breakdown, struktur transverse pada domain wall mengalami perubahan menjadi struktur vortex/anti-vortex.

Kata kunci: domain wall, nanowire, medan Walker breakdown, struktur transverse, struktur vortex/anti-vortex.

ABSTRACT

Name   : Andy Sumarta

Title   : Micromagnetic Study Magnetic Domain Wall Dynamics on Permalloy Nanowires ($Ni_{80}Fe20$)

We have investigated the domain wall dynamics in Permalloy material with nanowire shape using public micromagnetic simulation software, OOMMF based on the Landau-Lifshitz-Gilbert equation. We have observed domain wall dynamic for different thickness and width respect to external magnetic field. Domain wall velocity increases as the external magnetic field increase and abruptly decreases after critical field which is called Walker breakdown field. Before Walker breakdown, domain wall moving while keeping transverse inner structure, and after Walker breakdown, transverse inner structure transform to vortex/anti-vortex inner structure.

Keywords: domain wall, nanowire, Walker breakdown field, transverse inner structure, vortex/anti-vortex inner structure

CONTENTS

LIST OF FIGURES

Chapter 1
INTRODUCTION

1.1 Background

Recently, development of electronic devices based on spin properties become increasing after the discovery the GMR effect by Ferth and Grunberg in 1988 [1,2]. With the manipulation of intrinsic electron spin configuration is used to store information data bit rather than conventional electron charge. This achievement offers a breakthrough in the spin based electronics devices such as spintronics devices and magnetic memory logic which invoke the interaction between spin and magnetic properties of materials [3-6]. One of potential materials for magnetic memory is ferromagnetic nanowire.

Over decade, the investigation DW dynamic on ferromagnetic nanowire becomes intensive study both experiment or simulation. For example, the racetrack memory (RM) where the information data bit based on DWs dynamic along ferromagnetic nanowire[3-5]. Numerous study has been reported the DW dynamics in straight wire driven by external magnetic field [7-9]. Depending on the external field, DW moves with or without changing its inner structure [8,9]. It is found that the DW velocity increases while keeping inner structure to be a transverse wall type as external magnetic field increased until reaching Walker breakdown field. After Walker breakdown field, DW velocity drop suddenly [10,11]. The DW motion becomes more complex in this field region, and inner structure of DW exhibit a vortex/antivortex wall type.

Several investigations have been reported that the DW motion depends on the thickness, width and material parameters of the sample [9,12]. Using variation of width and thickness, the inner structure such as transverse and vortex/anti-vortex is represented by a phase diagram. This means that the DW inner structure plays an essential role in governing DW dynamics in ferromagnetic nanowires. By introducing a notch into ferromagnetic nanowires, DW propagation can be controlled. An investigation about

notched ferromagnetic nanowires showed asymmetric ground state spin configuration of transverse DW [13]. This investigation could be very essential in designing spin based devices utilizing the DW behavior. Another observation showed the DW collision around the Walker breakdown [14]. This DW collision was inevitably involved in such devices using DW motion. This collision leading to annihilation of DWs and can be used for magnetic bit switching in devices.

The most sample of ferromagnetic nanowire in the present studies of DW dynamic behaviour are Permalloy ($Ni_{80}Fe_{20}$). Because permalloy is isotropic magnetic material and then anisotropy energy can be set to zero for simplicity. Permalloy also has showed a low coercivity property that essential in switching magnetization process.

1.2 Purposes

The main purpose of this study is the investigation of DW dynamics on Permalloy nanowires by means of micromagnetic simulation. In this study, we observe DW velocity and DW inner structure with respect to thickness and width variation.

1.3. Organization of thesis

This thesis is organized as follows:

Chapter 1 represents some review of DW dynamics in ferromagnetic nanowires for spin based devices application such as racetrack memory, the main purpose for this study and the organization of this thesis.

Chapter 2 represents a brief theory such as magnetic domain, domain wall, and magnetic energy contribute in the magnetic system. Landau-Lifshitz-Gilbert equation is fundamental equation for magnetization dynamic of magnetic moment in ferromagnetic.

Chapter 3 describes the micromagnetic simulation procedure. We examine some important parameter for simulation, that is geometry of sample, cell size, damping parameter, material parameters, and the strength of external field. In this work, we perform the micromagnetic simulation by means of public

micromagnetic simulation software, OOMMF. We investigate a dynamic behavior under the applied field, such as DW velocity and DW inner structure corresponds to width and thickness variation.

Chapter 4 examines the investigation DW dynamics both static and dynamics behavior on Permalloy nanowires, inner structure, and energy profiles.

Chapter 5 the end of this thesis which give the conclusions of this work and the prospect for the future.
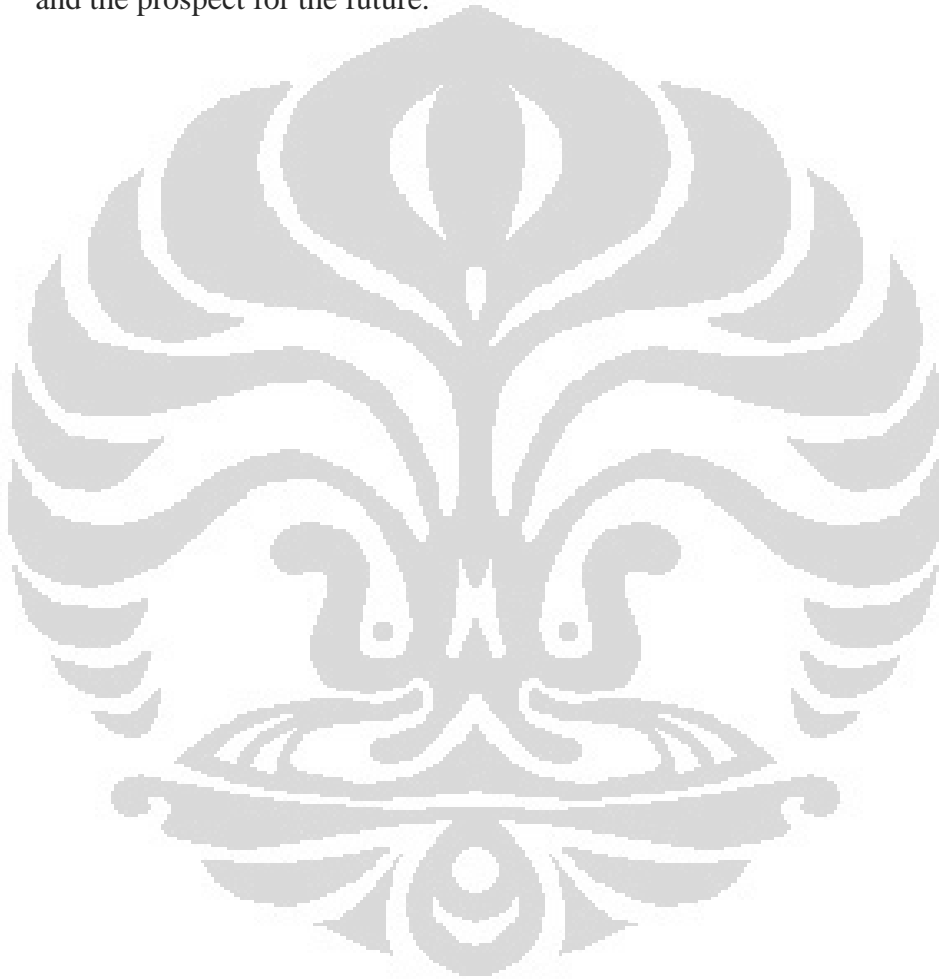
Chapter 2
THEORY

In this chapter, we briefly describes the theory which is related for the study. We introduce the basic concept of magnetization dynamic in ferromagnetic materials driven by external magnetic field. Magnetization experience dynamic precession that was first proposed by Landau-Lifshitz in 1935 and modified by Gilbert in 1955, which is called Landau-Lifshitz-Gilbert equation. Then we discuss about magnetic domain where magnetic moment in this region are aligned parallel to each other even without external field. The transition between this region is called magnetic domain wall. Domain wall is consequence of competition between exchange energy and anisotropy energy in which to reach minimum energy of domain wall. Commonly there are two types of domain wall structure. Bloch wall is preferable in bulk materials and Néel wall is mostly favorable in thin films materials.

2.1 Magnetization dynamic

The basic principle in magnetism is the magnetic moment. In the view of classical magnetism, the magnetic moment was governed by rotating electric charge. If there is a current I around an infinitely small area d$\mathbf{A}$ (loop), then the magnetic moment $d\boldsymbol{\mu}$ is given by

$$d\boldsymbol{\mu} = Id\mathbf{A} \qquad (2.1)$$

The magnitude of vector d$\mathbf{A}$ is equal to the area of the loop and has a direction that is determined by the direction of the current around the loop. The magnetic moment vector $d\boldsymbol{\mu}$ points normal to the plane of the loop and can be either parallel or antiparallel with angular momentum vector. If the current come from the negative charge stream, then the magnetic moment vector will be have antiparallel direction respect to angular momentum vector.

Let's consider a ring with area $S = \pi r^2$ as illustrated in figure 2.1. The current produced by an electric charge q taking round this area with frequency ω is $I = q\omega / 2\pi$. The magnetic moment produced by electric charge rotation can be written as

$$\boldsymbol{\mu} = \frac{q}{2} r^2 \boldsymbol{\omega} = -\frac{e}{2} \mathbf{r} \times \mathbf{v} \qquad (2.2)$$
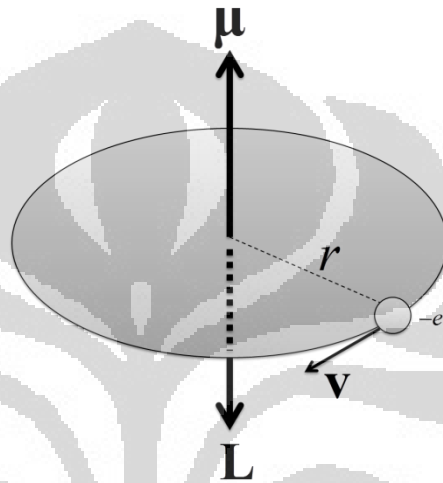
Figure 2.1 The magnetic moment produced by moving electron charge around the loop with radius r, velocity $\mathbf{v}$ and angular momentum ω. For electron, the direction of angular momentum $\mathbf{L}$ is opposite to magnetic moment.

Where the electron charge of $q = -e$ and vector relation between angular frequency and velocity is $\mathbf{v} = \boldsymbol{\omega} \times \mathbf{r}$. From classical angular momentum equation, we have $\mathbf{L} = m_e (\mathbf{r} \times \mathbf{v}) = m_e \omega^2 \mathbf{r}$, thus equation (2.2) can be express as

$$\boldsymbol{\mu} = -\frac{e}{2m_e} \mathbf{L} \qquad (2.3)$$

According to Bohr atom model, the magnitude of the angular momentum of electron in the ground state must be equal $\hbar$, so the magnitude of angular momentum is

$$\mu = -\frac{e}{2m_e}\hbar \qquad (2.4)$$

Where the quantity of $\gamma = \frac{e}{2m_e}$ is known as gyromagnetic ratio of electron. As we can see, this quantity is the constant of proportionality which connects between angular momentum and magnetic moment.

When magnetic field applied, there is a torque that will be act on magnetic moment in a perpendicular direction with it. This torque caused the magnetic moment precesses around magnetic field direction. This torques related to angular momentum by Newton's classical equation of motion

$$\mathbf{T} = \frac{d\mathbf{L}}{dt} = \mathbf{\mu} \times \mu_0 \mathbf{H} \qquad (2.5)$$

And then, with equation (2.5) we established equation of motion for a magnetic moment $\mathbf{\mu}$ respect to external magnetic field $\mathbf{H}$

$$\frac{d\mathbf{\mu}}{dt} = -\frac{e}{2m_e}\left(\mathbf{\mu} \times \mu_0 \mathbf{H}\right) = -\gamma \mu_0 \left(\mathbf{\mu} \times \mathbf{H}\right) \qquad (2.6)$$

This equation gives a consideration without damping process. As an important result, we can see that, magnetic moment only experience precession and not to rotate toward external field direction.

In Landau-Lifshitz-Gilbert equation [15], damping of precession motion was introduced. We can analogous this damping precession motion as dissipative motion. The dissipative term is proportional to time derivatives of the magnetization and add to the effective field $\mathbf{H}_{eff}$. This dissipative term slow down the magnetic moment motion and tend to align magnetic moment parallel with $\mathbf{H}_{eff}$, then equation (2.6) can rewrite as

$$\frac{d\mathbf{M}}{dt} = -\gamma \mathbf{M} \times \left(\mathbf{H}_{eff} - \eta \frac{d\mathbf{M}}{dt}\right) \qquad (2.7)$$

Where η is positive constant and a damping constant $\alpha = \gamma M \eta$. We obtain

$$\frac{d\mathbf{M}}{dt} = -\gamma \mathbf{M} \times \mathbf{H}_{eff} + \frac{\alpha}{M} \mathbf{M} \times \frac{d\mathbf{M}}{dt} \tag{2.8}$$

Multiplying equation (2.8) by $\mathbf{M} \times$, it gives

$$\mathbf{M} \times \frac{d\mathbf{M}}{dt} = -\gamma \mathbf{M} \times \left(\mathbf{M} \times \mathbf{H}_{eff} \right) + \frac{\alpha}{M} \mathbf{M} \times \left(\mathbf{M} \times \frac{d\mathbf{M}}{dt} \right) \tag{2.9}$$

Using the vector relationship: $\mathbf{M} \times \left(\mathbf{M} \times \frac{d\mathbf{M}}{dt} \right) = \left(\mathbf{M} \cdot \frac{d\mathbf{M}}{dt} \right) \mathbf{M} - M^2 \frac{d\mathbf{M}}{dt}$ in the second term of equation (2.9), we obtain

$$\mathbf{M} \times \frac{d\mathbf{M}}{dt} = -\gamma \mathbf{M} \times \left(\mathbf{M} \times \mathbf{H}_{eff} \right) + \alpha M \frac{d\mathbf{M}}{dt} \tag{2.10}$$

Substitute equation (2.10) in to equation (2.8), we obtain the Landau-Lifshitz-Gilbert equation

$$\frac{d\mathbf{M}}{dt} = -\frac{\gamma}{\left(1+\alpha^2\right)} \mathbf{M} \times \mathbf{H}_{eff} - \frac{\gamma\alpha}{\left(1+\alpha^2\right)M} \mathbf{M} \times \left(\mathbf{M} \times \mathbf{H}_{eff} \right) \tag{2.11}$$

The first term on the right hand side of equation (2.11) represents gyromagnetic precession and the second term represents the damping effect of the precession [16]. For small α, the term $\left(1+\alpha^2\right)$ is equal to one and the equation reduce to Landau-Lifshitz equation.

2.2 Magnetic domain and domain wall

In the year 1907, P. Weiss stated that in the ferromagnetic materials, there are a number of small regions called *magnetic domain wall*. Each of domain walls exhibits the saturation magnetization. The magnetization direction of different domain need not be parallel. The existence of domains can be explains the observation of some ferromagnetic specimens about saturation of magnetization over the whole sample by the application of a very weak magnetic field. In this case, the applied field does not have to align magnetic

moment but merely to align the magnetic domain. It is also possible for the magnetization to be zero in the absent of magnetic field that is the manifestation of domains. In each domain, magnetization reach saturation, but different direction of magnetization in each domain cause the magnetization canceled out and giving zero magnetization.

The transition layer that separates domains is called domain wall. The domain wall can be classified by the angle between the magnetization in the two domains that is 180° domain wall and 90° domain wall. A 180° domain separates two with opposite magnetization whereas a 90° separates two domain that magnetization is perpendicular each other. These domains wall type is showed by figure 2.2
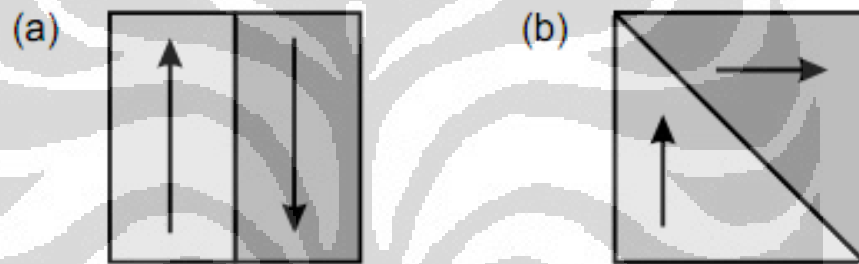

Figure 2.2. (a) 180° and (b) 90° domain wall [17].

In the Bloch wall proposed by F. Bloch, the change of the spin direction is not occur within discontinues jump across single atomic plane, but it happen within continues way over many atomic plane. Let us consider a 180° Bloch wall that is illustrated in figure 2.3.

For ferromagnetic materials, there is energy cost if the spins rotate and make an angle θ respect to each other. This spins interacts via exchange interaction and has an energy $-2j\mathbf{S}_1 \cdot \mathbf{S}_2 = -2jS_1S_2\cos\theta$. Their energy is $-2jS^2$ when $\theta = 0$. Hence the cost energy when $\theta \neq 0$ is approximately $jS^2\theta^2$ if $\theta \ll 1$. The spins rotate through N sites by an angle π. Hence the energy cost is equal to N contribution of $jS^2\theta^2$ through all sites, this exchange energy can be writing as

$$E_{ex} = \frac{jS^2\pi^2}{N} \qquad (2.12)$$

Where $\theta = \frac{\pi}{N}$. We are interested in γ_{ex}, the exchange energy per unit area of the wall. With the simple cubic structure with the lattice constant a, the exchange energy per unit area of the transition layers is

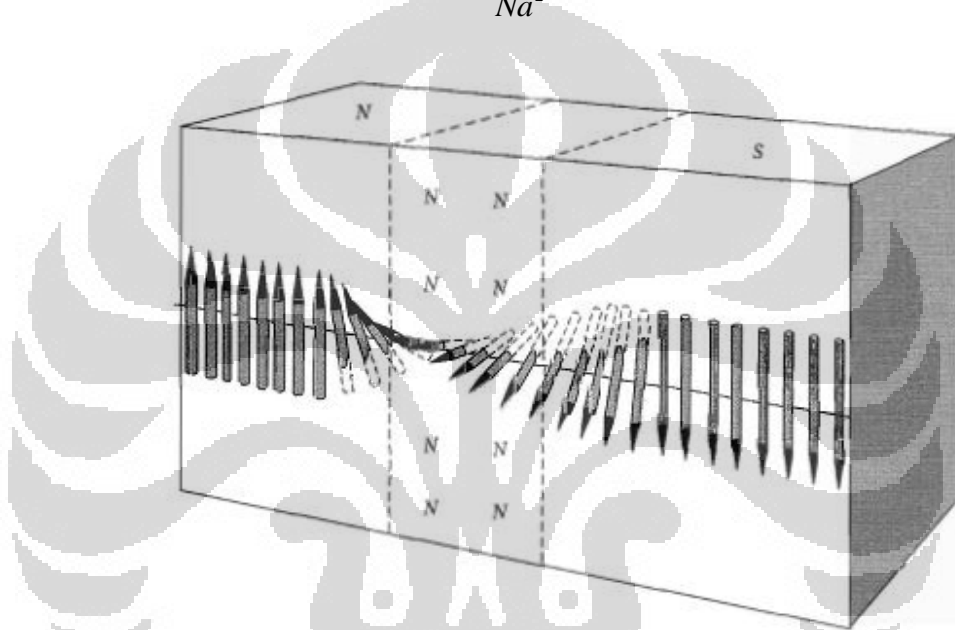$$\gamma_{ex} = jS^2 \frac{\pi^2}{Na^2} \qquad (2.13)$$

Figure 2.3. The structure of 180° Bloch wall where the spin rotate in a gradual way over many atomic planes inside domain wall [18].

Exchange energy decreases as N increases. This result indicates that exchange interaction caused domain wall growing in size through the entire system. Therefore domain wall will be untwisting until another interaction stops them. Another interaction is magnetocrystalline anisotropy. This interaction refers to anisotropy energy that will be act to limit domain wall size. At this point, the actual thickness of domain wall can be determined from the minimization of exchange and anisotropy energy. For a simple cubic crystal structure, the anisotropy energy is

$$\gamma_{ani} = KNa \tag{2.14}$$

With anisotropy constant K and the domain wall energy γ_{DW}

$$\gamma_{DW} = \gamma_{ex} + \gamma_{ani} = \frac{jS^2\pi^2}{Na^2} + KNa \tag{2.15}$$

The minimization energy is satisfied when

$$\frac{\partial\gamma_{DW}}{\partial N} = -\frac{jS^2\pi^2}{N^2a^2} + Ka = 0 \tag{2.16}$$

Solving equation (2.16) we obtain

$$N = \pi\sqrt{\frac{jS^2}{Ka^3}} \tag{2.17}$$

Therefore the thickness of domain wall is given by

$$\delta = Na = \pi\sqrt{\frac{jS^2}{Ka}} = \pi\sqrt{\frac{A}{K}} \tag{2.18}$$

And the domain wall energy γ_{DW} is obtained

$$\gamma_{DW} = \pi\sqrt{\frac{jS^2K}{a}} + \pi\sqrt{\frac{jS^2K}{a}} = 2\pi\sqrt{\frac{jS^2K}{a}} \tag{2.19}$$

Where A is the exchange stiffness constant and depending on the lattice structure. In the case of simple cubic lattice $A = jS^2/a$, the body center cubic lattice $A = 2\,jS^2/a$ and for the face center cubic lattice $A = 4\,jS^2/a$.

For thin film ferromagnetic materials, domain wall prefer to lie in the plane. This different structure is form in order to minimize the magnetostatic interaction of magnetic free pole at the surface. This structure is called Néel wall and illustrated in figure 2.4.
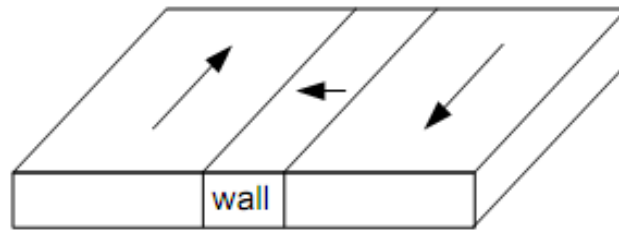
University of Indonesia

Figure 2.4 structure of Néel wall. This type of domain wall is preferred in thin film ferromagnetic [19].

When the geometry changes from bulk to nanoscale materials, the formation of domain wall not only affected by intrinsic materials properties, but also affected by the geometry of the materials. Like in nanowires, magnetostatic energy leads to an alignment of the magnetization with the edge of the structure in order to minimize the magnetostatic energy [24].

When a domain wall formed in the nanowire, then two domains with opposite direction exist. This configuration is depicted in figure 2.5. A domain wall has to be present to separate two domains and called 180° head to head domain wall [24].
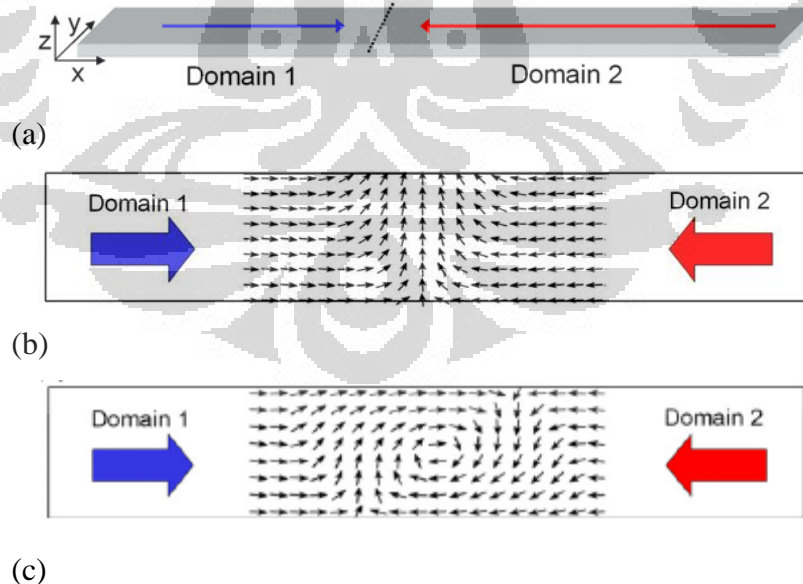

Figure 2.5 (a) Sechematic of nanowire with two opposite domain direction, (b) Structutre of transverse 180° head to head DW, (c) Structutre of transverse 180° head to head DW [24].

In experiment, this magnetic structure is observed using magnetic force microscopy (MFM). Figure 2.6 show the magnetic structure for permalloy [3]. We can observed transverse DW structure in part (a) and vortex DW structure in part (b). The magnetic structure weather transverse or vortex DW structure is strong dependent on nanowire geometry.

(a)   (b)

Figure 2.6 Magnetic structure of permalloy nanowire observed using MFM (a) transverse DW structure, (b) vortex DW structure [3].

Chapter 3
MICROMAGNETIC SIMULATION

3.1 Micromagnetic systems

In this work, the micromagnetic simulation were carried out by assuming rectangular shape Premalloy ($Ni_{80}Fe_{20}$) using public micromagnetic simulation software, OOMMF based on Landau-Lifshitz-Gilbert equation [20]. Finite difference method was used to solve the discretized three dimensional problems. Discretization of the system was achieved by using square grids over a region where magnetization is constrained to be uniform in this discretize region. The name of the three dimensional solver is OXS (OOMMF extensible solver). OOMMF employs the finite different method to solve Landau-Lifshitz-Gilbert equation which requires discretization over a grid of cell. Inside the discretize region, magnetization is constrain to be uniform through the thickness of nanowire. The cell size used for computation will be choosing by computation time and memory consumption consideration. Ideally, the cell size must be smaller than the relevant length, that is exchange length $l_{ex} = \sqrt{2A / \mu_0 M_s^2}$ which is describes the competition between interatomic exchange and magnetostatic self interaction [21]. The material parameters corresponding to Permalloy used throughout this micromagnetic simulation is saturation magnetization $M_s = 8 \times 10^5$ A/m, the exchange stiffness constant $A = 13 \times 10^{-12}$ J/m and magneto-crystalline is zero

3.2 Micromagnetic simulation procedure

In the simulation of DW dynamics, the length of the wire is 2000 nm, the width is varied to be 100 nm, 150 nm, and 200 nm whereas the thickness is varied to be 2.5 nm and 5 nm. The cell size of the simulation used for this simulation is $5 \times 5 \times t$, and damping constant α is set to be 0.01. The dimension and geometry of the wire is depicted in figure 3.1
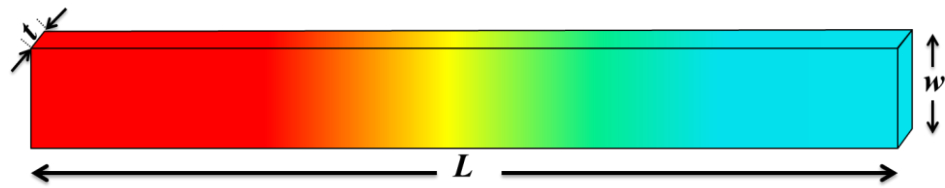
13

Figure 3.1 Dimension of nanowire which is used for this simulation the length of the wire is 2000 nm, the width is varied to be 100 nm, 150 nm, and 200 nm whereas the thickness is varied to be 2.5 nm and 5 nm.

Initially DW is set to be transverse structure with head to head configuration at middle of the wire. Then the system has been relaxed and leaved to reach equilibrium state in the zero external fields. The equilibrium state is illustrated in figure 3.2
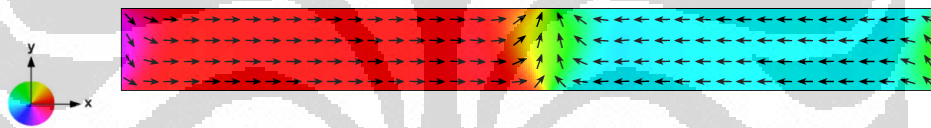

Figure 3.2 The equilibrium state of nanowire system with transverse structure. Arrow indicate the direction of magnetization in discretization region.

After the system reach equilibrium state, external magnetic field is applied using pulse field in the $+x$ direction with the rise time 0.1 ns and applied field duration for this pulse field is 1 ns. After 1 ns, pulse field is turned off and DW is leaved to be moved under zero external magnetic field.

4.1 DW motion in nanowire

We have observed DW motion inside nanowire under external magnetic field. When the pulse field is turn on and applied to a single DW in nanowire, the DW propagates like an independent entity as a classical Newtonian particle toward field direction and has a velocity that dependent with nanowire geometry and the strength of external magnetic field.

In principle, the DW velocity increase linearly with external field, the stronger external field, the faster DW motion. This characteristic is confirmed by several snapshot of nanowire depicted in figure 4.1 and figure 4.2
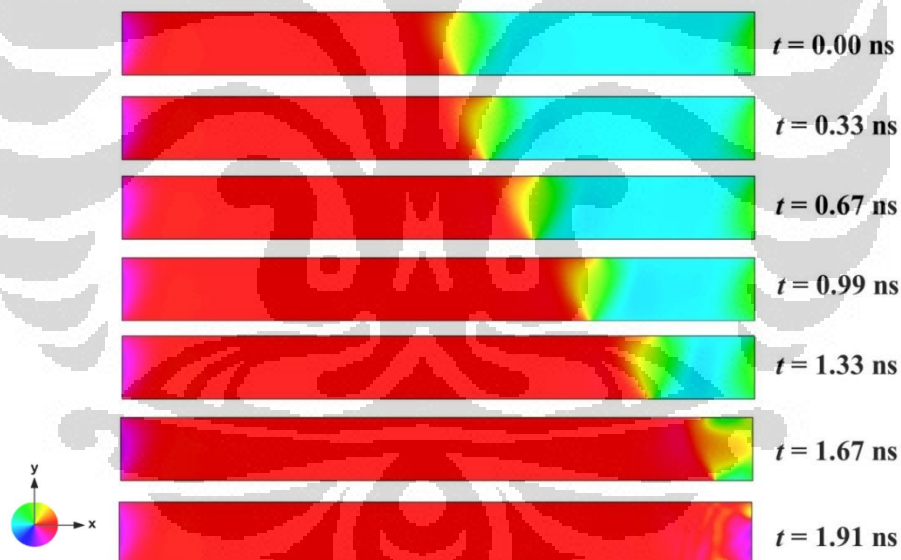

Figure 4.1 Evolutions of DW position in nanowire with thickness 5 nm and width 200 nm under external field 1 mT.
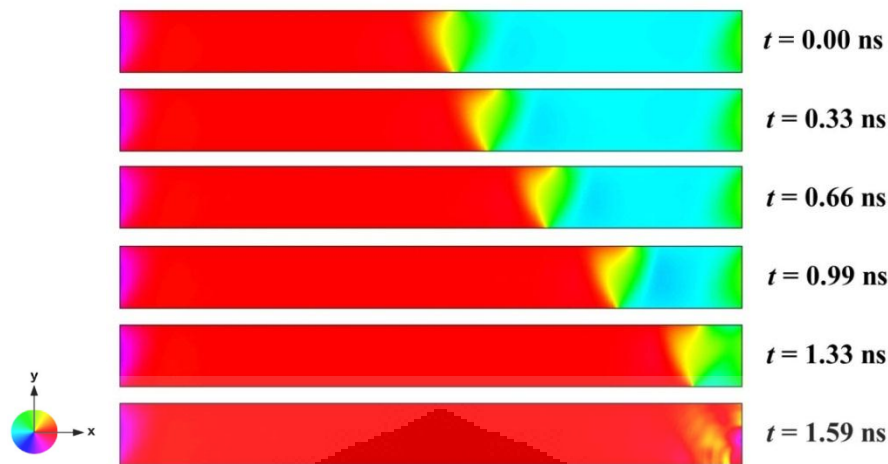
Figure 4.2 Evolutions of DW position in nanowire with thickness 5 nm and width 200 nm under external field 1.5 mT.

As we can see, DW that propagate in the nanowire under 1.5 mT field is more faster than nanowire under 1 mT field (544 m/s for 1 mT and 660 m/s for 1.5 mT) and achieve complete saturation of magnetization within 1.59 ns while 1.91 ns for nanowire under 1 mT field. From this figure, we can also see that, inner structure of DW didn't change and keep transverse during propagate toward external field. DW velocity increase up to 701 m/s under external field 1.8 mT. We expect that external field above 1.8 mT will be drive DW with faster velocity, however we observe that the velocity of DW under external field above 1.8 mT decrease abruptly. This is the typical characteristic of Walker Breakdown field. In this case, external field 1.8 mT play role as Walker breakdown field. Such remarkable decrease of the velocity of DW is known to be associated with the oscillatory turbulent motion of DW. For compare to DWs motion in nanowire below Walker Breakdown field, we give several snapshots of DW motion in nanowire under 3 mT fields in figure 4.3.
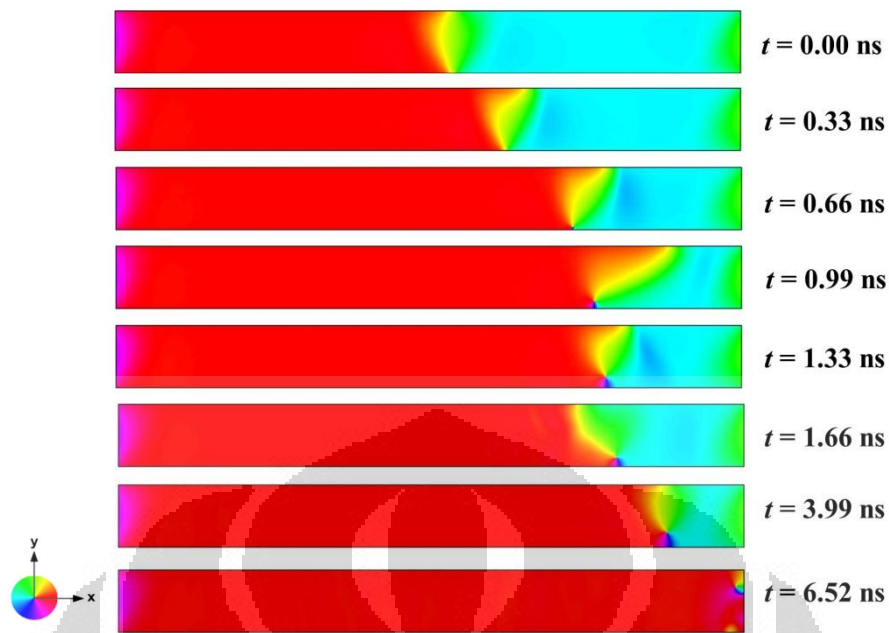
Figure 4.3 Evolution of DW position in nanowire with thickness 5 nm and width 200 nm under 3 mT field.

Above this Walker breakdown field, DW moves slowly and experience oscillation motion with average velocity 122 m/s. More interesting, DW inner structure change from transverse to anti vortex when propagating. We can see at the figure 4.3, the change of inner structure of DW is start from appearance of anti vortex nucleation at the bottom edge of the wire, with the core moments pointing in the $-z$ direction ($t = 0.72$ ns). The nucleated anti vortex seen to cross the width of the nanowire and producing a turbulent motion of DW that leading to lower average domain wall velocity [22].

For the higher field, for example at $B = 6$ mT, more complicated domain wall structure were observed (figure 4.4). Besides nucleation of anti-vortex, we found there is vortex nucleation at $t = 0.41$ ns and followed by annihilation of anti-vortex after pulse field has been tuned off.
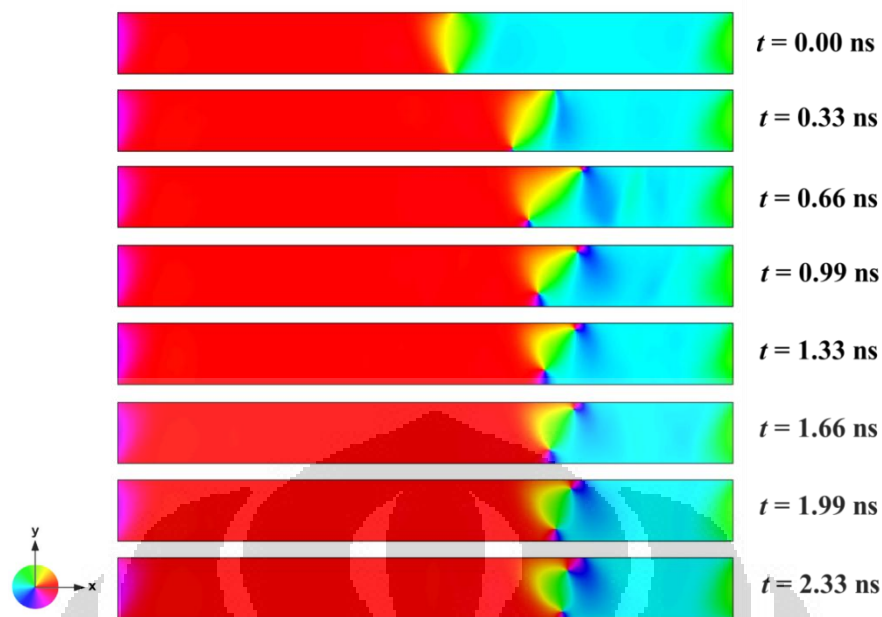
Figure 4.4 Evolution of DW position in nanowire with thickness 5 nm and width 200 nm under 6 mT fields.

4.2 DW position and velocity in nanowire

The position of domain wall respect to time for various geometry of nanowire is showed from figure 4.5 to figure 4.10. For nanowire with thickness 2.5 nm and width 100 nm, gradient of DW position showed constant value in small applied pulse field of 1 mT – 3.3 mT. And we also observed that, the gradient increase which means, average velocity increase with the magnitude of pulse field. But, above 3.3 mT, that is 3.5 mT – 7 mT, gradient of DW position decrease and become negative and caused the average DW velocity decrease abruptly. For this nanowire geometry, the magnitude of pulse field of 3.3 mT play role as Walker Breakdown field. The negative gradient indicates that DW propagates in the opposite direction with external pulse field for a moment. The consequence of this
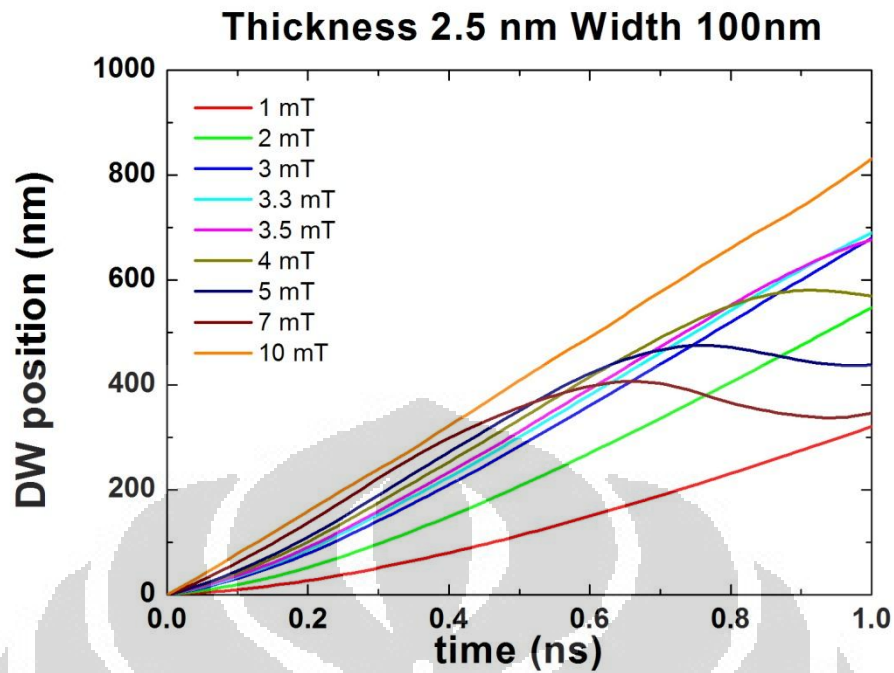
Thickness 2.5 nm Width 100nm

Figure 4.5 DW position respect to time for thickness 2.5 nm and width 100 nm.
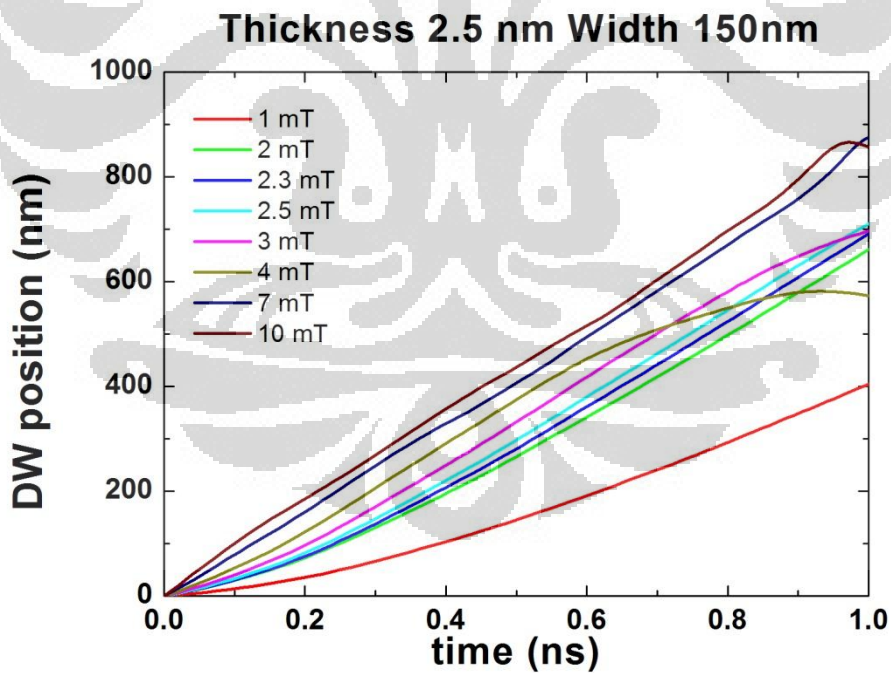
Thickness 2.5 nm Width 150nm

Figure 4.6 DW position respect to time for thickness 2.5 nm and width 150 nm.
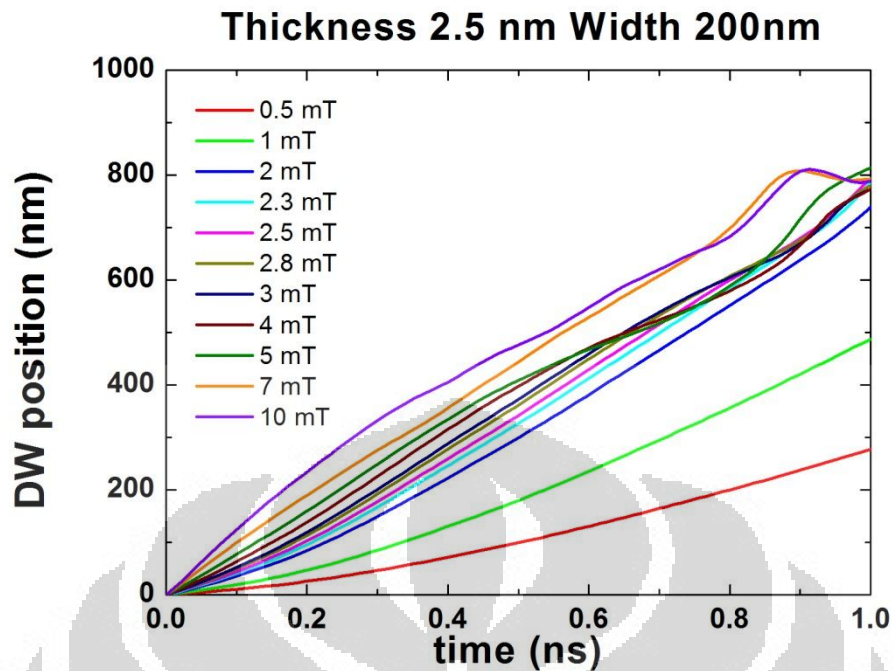
Figure 4.7 DW position respect to time for thickness 2.5 nm and width 200 nm.

DW motion is oscillatory motion during propagating [14, 22] as we mention before when DW structure changed from transverse DW to vortex/anti-vortex DW. For higher pulse field, 10 mT, gradient of DW showed a steeper curved compare to other external pulse field after Walker Breakdown field. This gives a higher average velocity for DW during propagating. This observation confirmed the DW characteristic when propagating under external magnetic field. DW velocity increase linearly with external field and keeping transverse inner structure until reaching Walker Breakdown field. After this Walker Breakdown field, DW velocity decrease abruptly and the inner structure changed to vortex/anti-vortex structure. And for high field, average DW propagates with faster velocity than other external pulse field after Walker Breakdown field [22]. As we can see, what is the value of Walker breakdown field and what is high field in order to DW propagate with faster velocity, is depend on nanowire geometry.
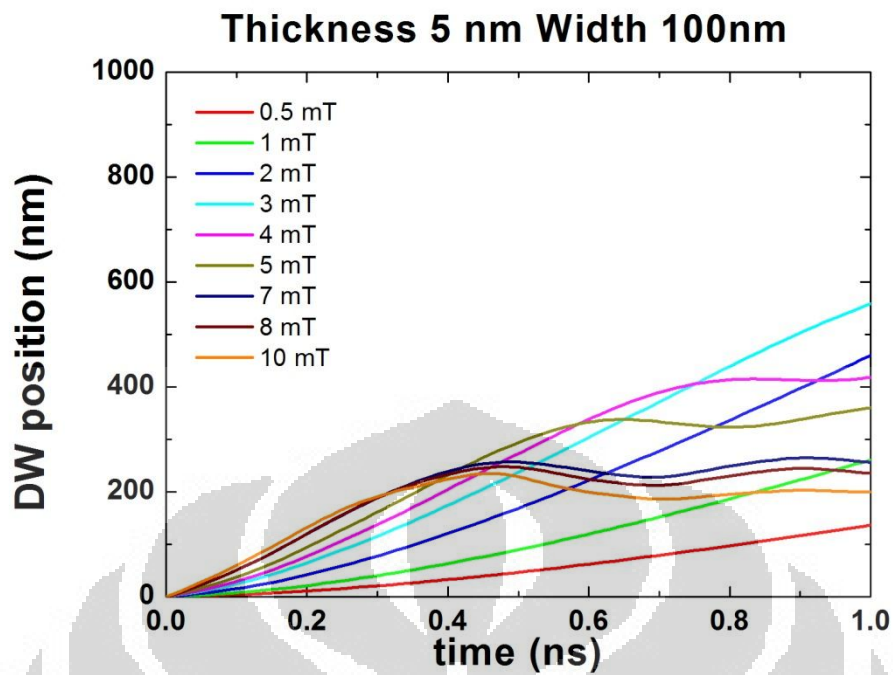
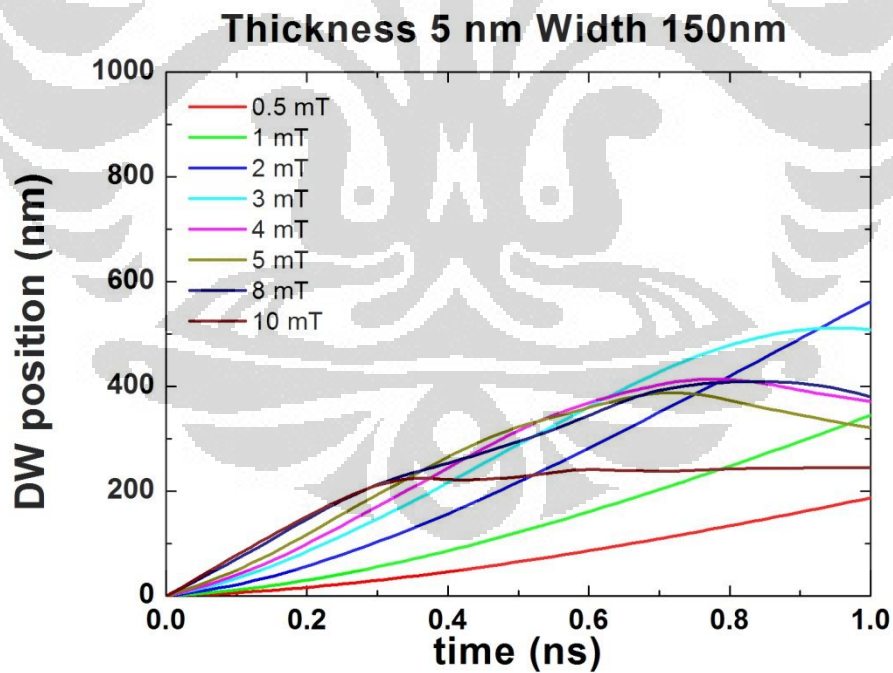Figure 4.8 DW position respect to time for thickness 5 nm and width 100 nm.

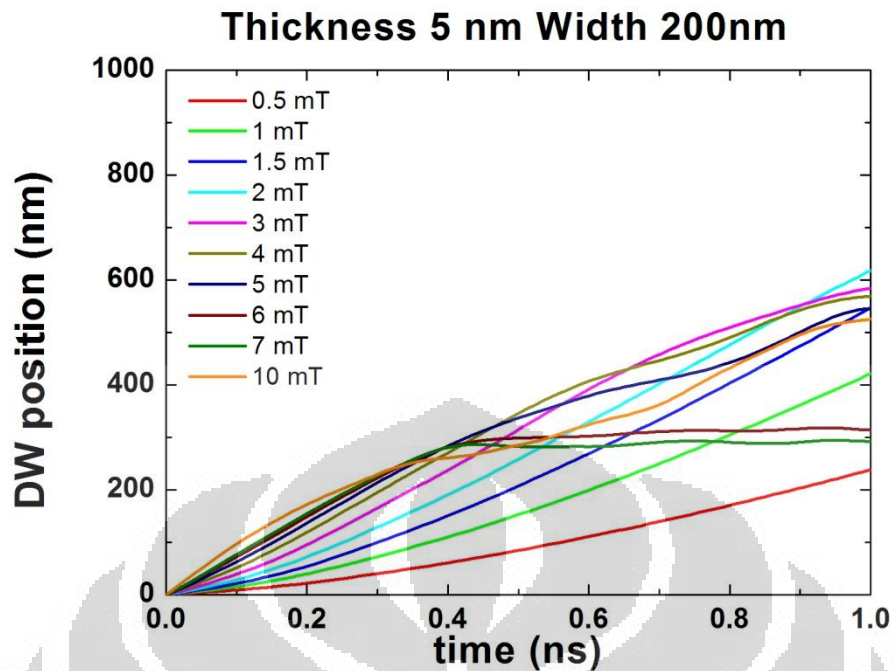Figure 4.9 DW position respect to time for thickness 5 nm and width 150 nm.

Figure 4.10 DW position respect to time for thickness 5 nm and width 200 nm.

For thicker nanowires (thickness 5 nm), the oscillation characteristic is more observable. Form figure 4.8 to 4.10, we can found that, during the pulse field is turn on within 1 ns, DW traveled shorter distances in nanowire with thickness 5 nm than thickness 2.5 nm. This observation gives information that DW propagate with lower average velocity in thicker nanowire and we will see later, this consideration is true when we compare DW velocity versus external field curve for various thickness.

As we mention before, the propagating velocity of DW is dependent to nanowire geometry. Not only propagating velocity of DW affected by nanowire geometry, but Walker breakdown field and inner structure of DW may differ by each other. Figure 4.11 and 4.12 shows the relation between external field strength and DW velocity and we can see how the shape of the curve may differ for different nanowire geometry.
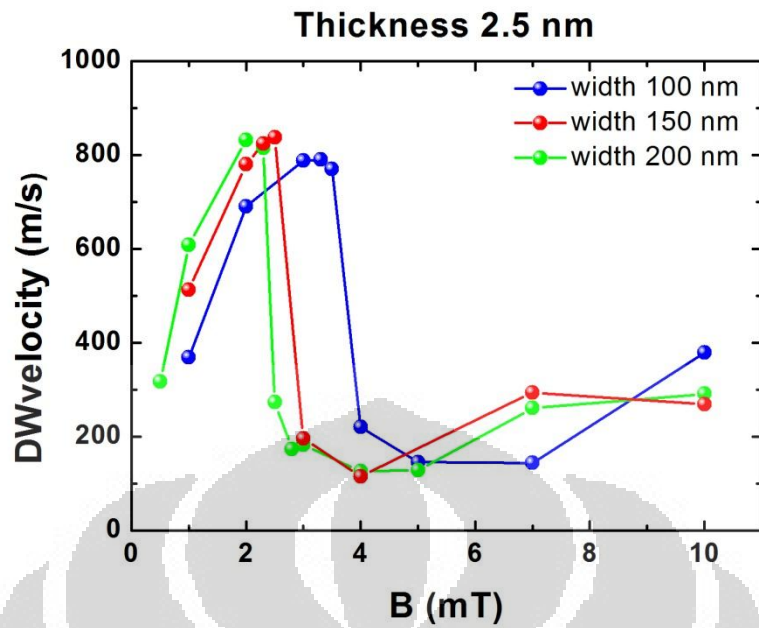
Figure 4.11 DW velocity respect to external field, nanowire with thickness 2.5 nm and variation width 100 nm, 150 nm, 200 nm.
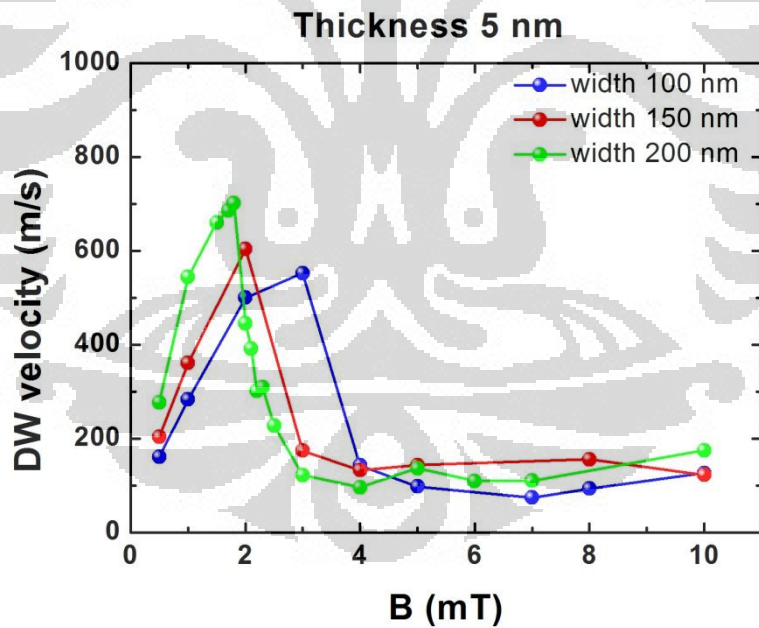

Figure 4.12 DW velocity respect to external field, nanowire with thickness 5 nm and variation width 100 nm, 150 nm, 200 nm.

Walker breakdown field decrease with increasing the width of the nanowire in each curve (thickness 2.5 nm and 5 nm). Also we observe that, before external field exceeding Walker breakdown field, DW velocity increase with increasing the width. This means at the wider nanowire, DW propagate with faster velocity, but this is valid until certain value of external field before Walker breakdown field. Walker breakdown field have a smaller value on the wider nanowire therefore anti vortex DW likely to be found on wider nanowire. In general view of figure 4.11 and 4.12, we found that DW velocity for nanowire with thickness 2.5 nm is greater than DW velocity in nanowire with thickness 5 nm. This is what we seen before when we compare distance traveled by DW in nanowire with thickness 2.5 nm and 5 nm. To confirm this observation, we plot velocity curve versus external field for each thickness in the same width parameters of nanowire in figure 4.13, 4.14, 4.15.
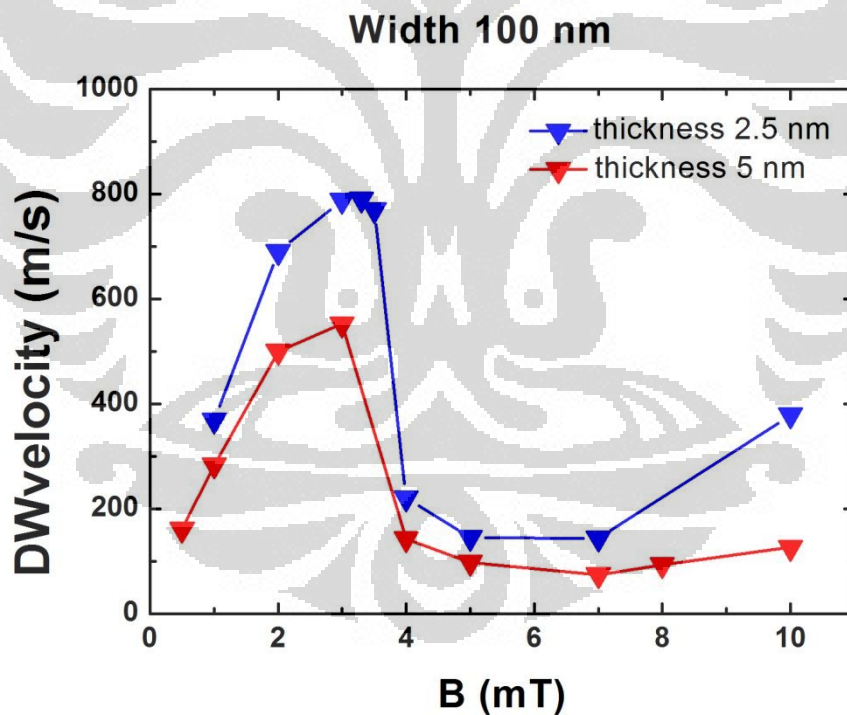

Figure 4.13 DW velocity respect to external field with variation thickness 2.5 nm, 5 nm for nanowire with width 100 nm.
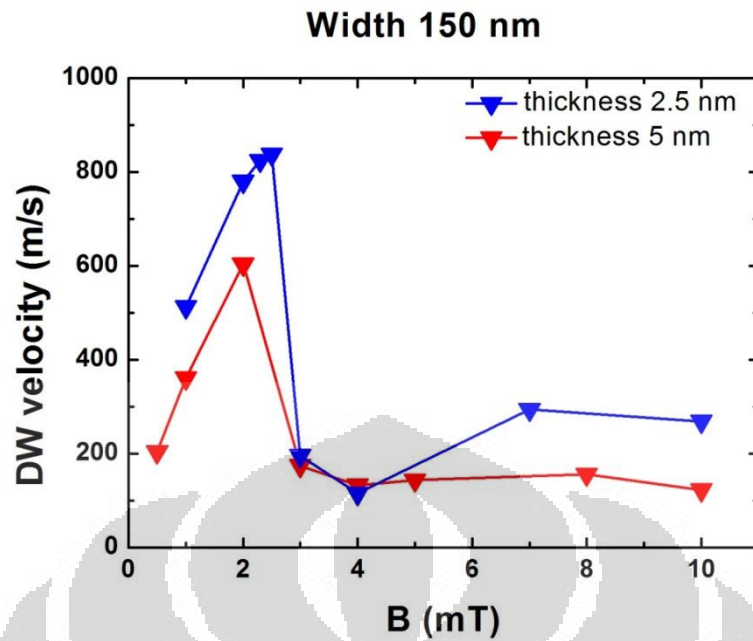
Figure 4.14 DW velocity respect to external field with variation thickness 2.5 nm, 5 nm for nanowire with width 150 nm.
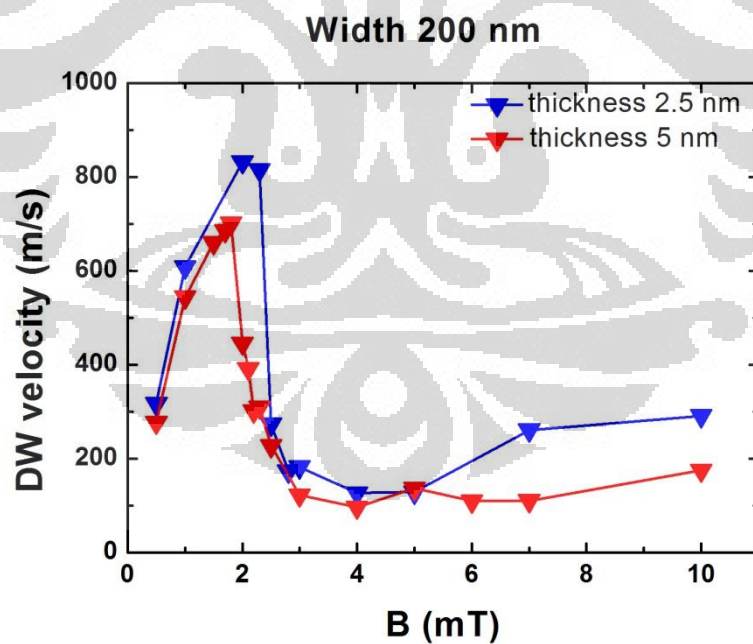

Figure 4.15 DW velocity respect to external field with variation thickness 2.5 nm, 5 nm for nanowire with width 200 nm.

From this figure we see that velocity and the Walker breakdown field decrease with increasing strip thickness. These results are reasonable because the magnetic moments in the wall acquire a component perpendicular to the nanowire plane by precession around the external field. This component gives a demagnetized field in perpendicular direction on plane of nanowire and then DW moves via the precession around this demagnetized field [9]. For compare to our result we give a result of simulated nanowire worked by Nakatani et al (ref [9]) in figure 4.16.
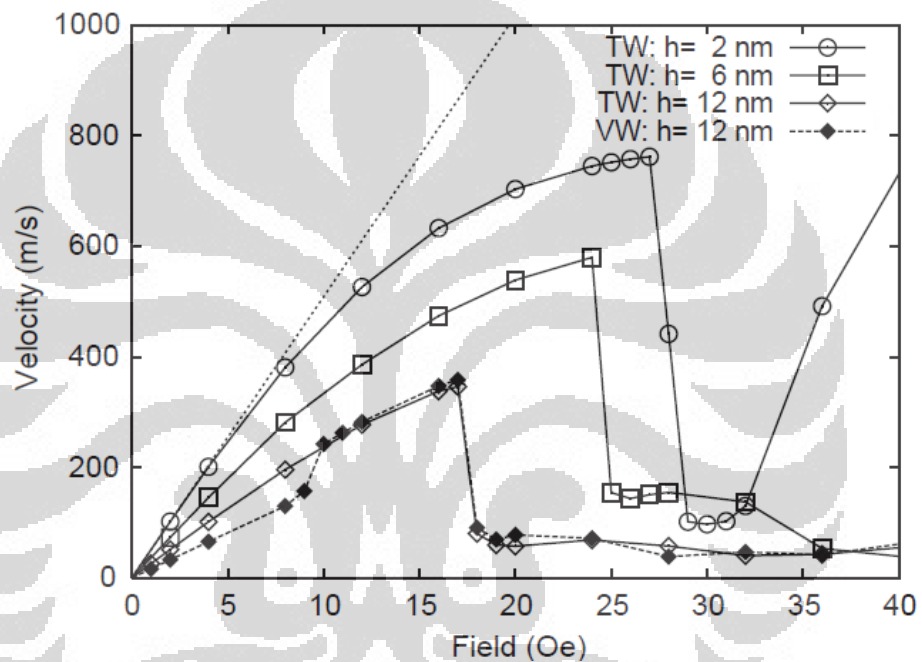

Figure 4.16 The result of simulated nanowire, simulated by Nakatani et al, DW velocity respect to external field with variation thickness.

We also give an experimental result from ref [23] in figure 4.17. The experiment is carried out using Permalloy strip .This result give the same characteristic, which is the magnitude of DW velocity increase linearly and after Walker Breakdown field, DW velocity decrease abruptly. Also we can see in this figure, DW velocity increase again linearly in high field region.
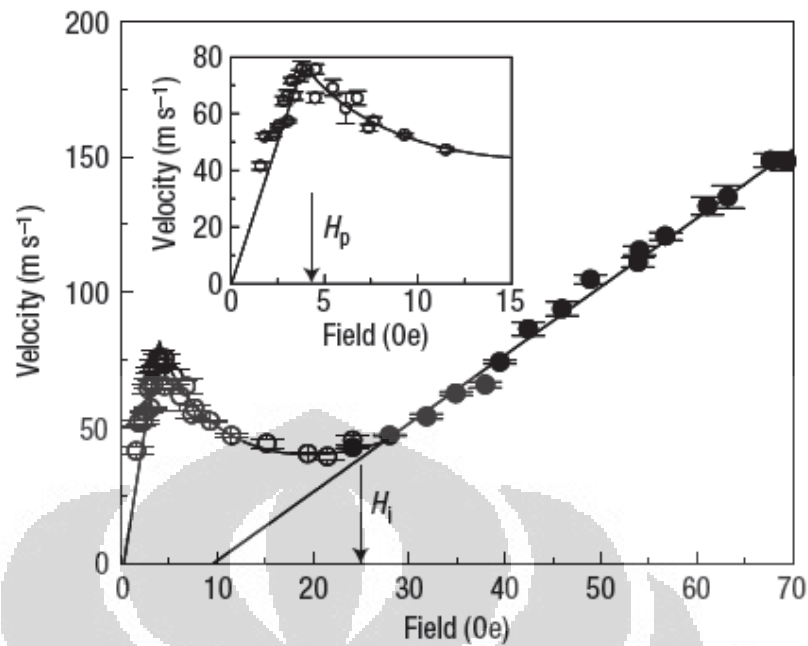
Figure 4.17 Experiment result performed by ref [23], domain wall velocity versus external field applied.

4.3 Analysis of energy term in simulated nanowire

Energy term play a role in formation of DW where the spin structure is a result of minimization energy. Without consideration of zeeman energy and anisotropies energy, the two important energy term are exchange energy and magnetostatic energy. If the exchange dominates, this will give a wider DW and if the magnetostatic dominates, the spins try to being parallel to the structure edge as much as possible yielding narrower DW [24].

To analyze detailed process during transformation, we have plot magnetic energies in figure 4.18 to figure 4.23. In general view, we can see that magnetostatic energy density is give greater contribution in total energy density than exchange density energy. For the case of steady motion of transverse DW structure, magnetostatic energy of the system didn't change too much, but for exchange energy, this energy term increase with external field applied. And also we observed that, for thicker and wider nanowire where DW has a tendency to transform to vortex wall, magnetostatic energy drop in significant value. For example, at nanowire with thickness 5 nm and width

200 nm, when external pulse field tuned to 6 mT, magnetostatic energy drop in significant value. If we referred to figure 4.4, the snapshots display the nucleation of vortex wall, in other word this drop value of magnetostatic energy caused by nucleation of vortex wall within nanowire. We observed the same characteristic for nanowire with thickness 5 nm and width 150 nm and then for nanowire with thickness 2.5 nm and width 200 nm we found extreme condition i.e. exchange energy become more dominant than magnetostatic energy.
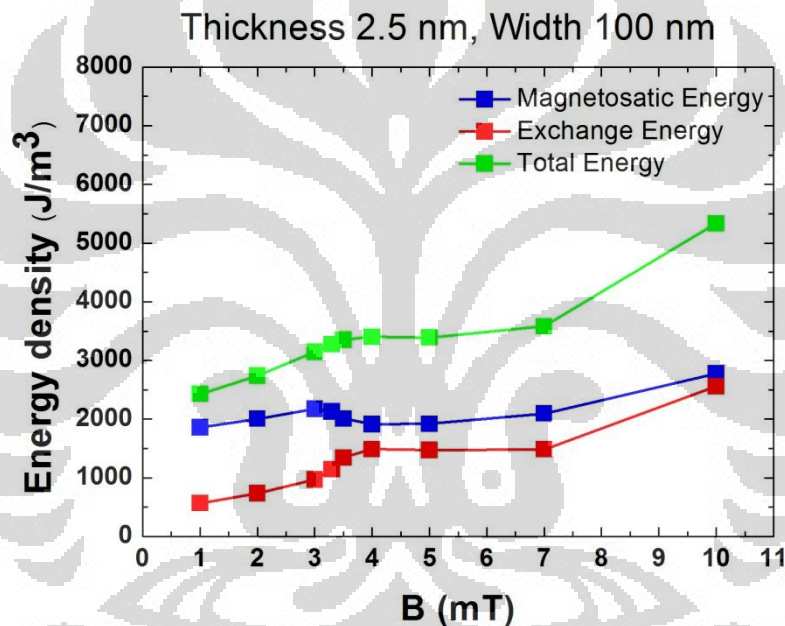
Figure 4.18 Magnetostatic and exchange energy density for simulated nanowire with thickness 2.5 nm and width 100 nm.
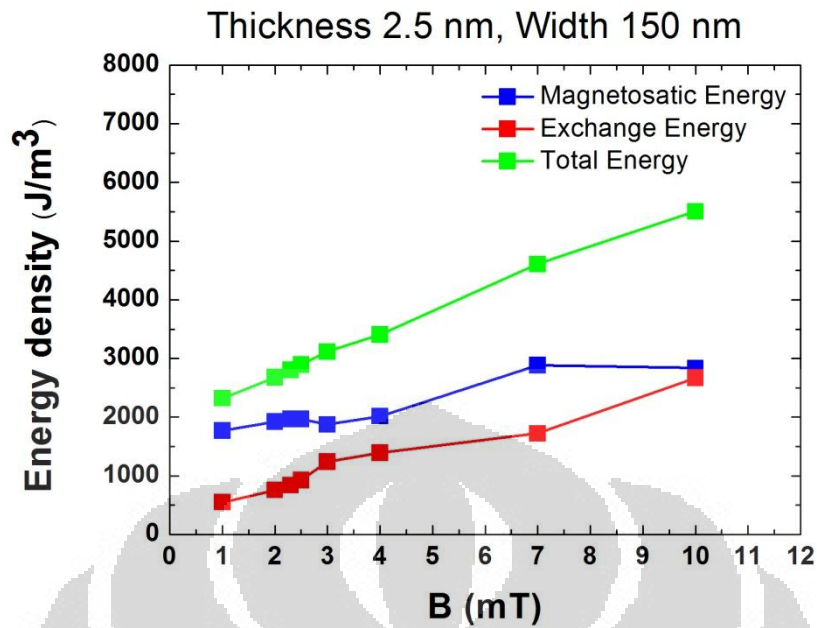
Figure 4.19 Magnetostatic and exchange energy density for simulated nanowire with thickness 2.5 nm and width 150 nm.
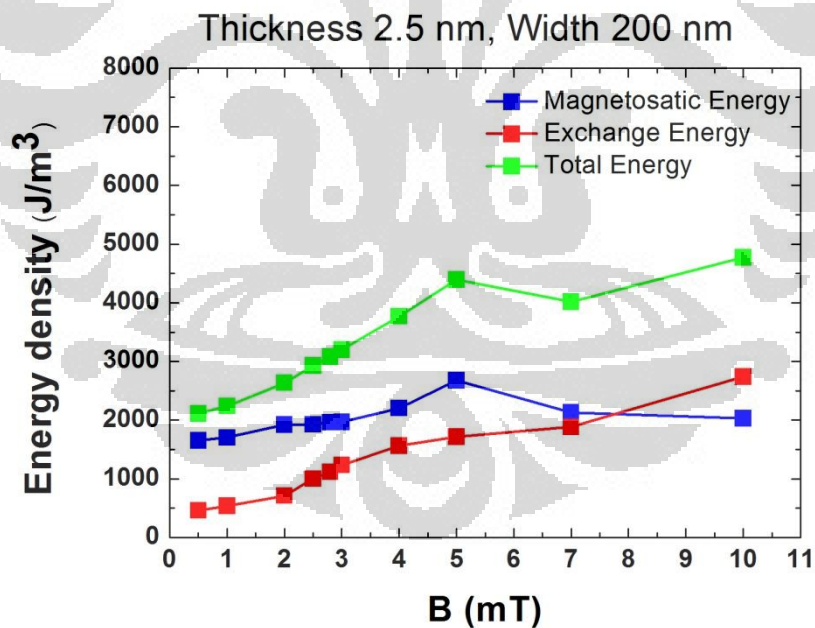

Figure 4.20 Magnetostatic and exchange energy density for simulated nanowire with thickness 2.5 nm and width 200 nm.
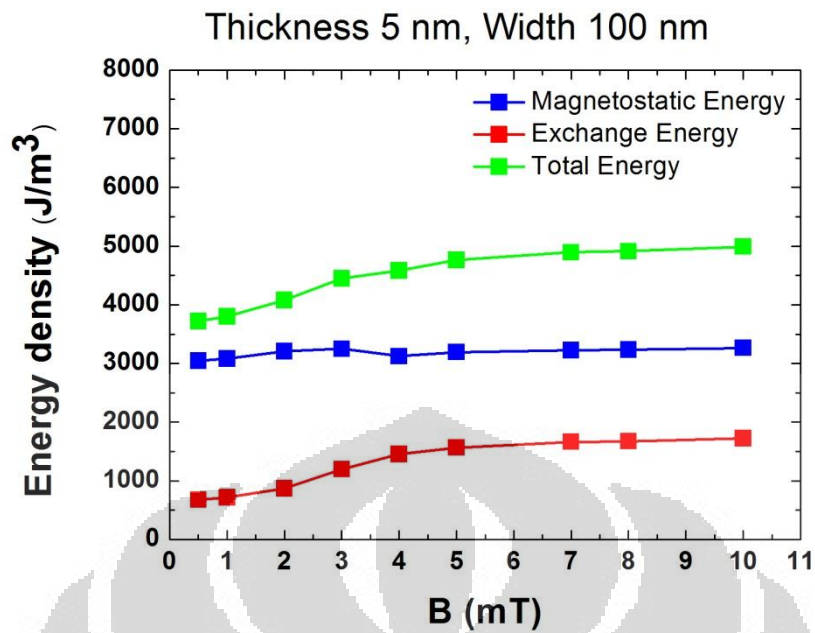
Figure 4.21 Magnetostatic and exchange energy density for simulated nanowire with thickness 5 nm and width 100 nm.
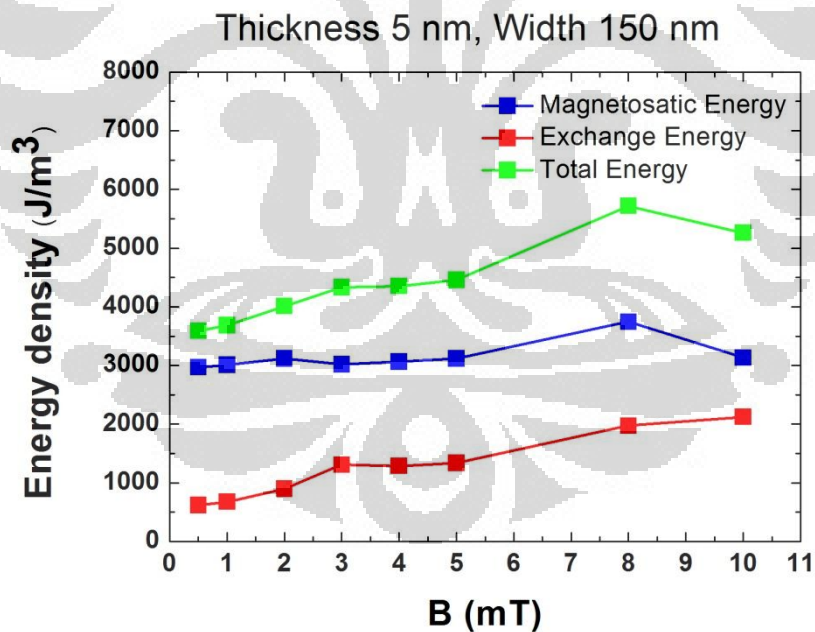

Figure 4.22 Magnetostatic and exchange energy density for simulated nanowire with thickness 5 nm and width 150 nm.
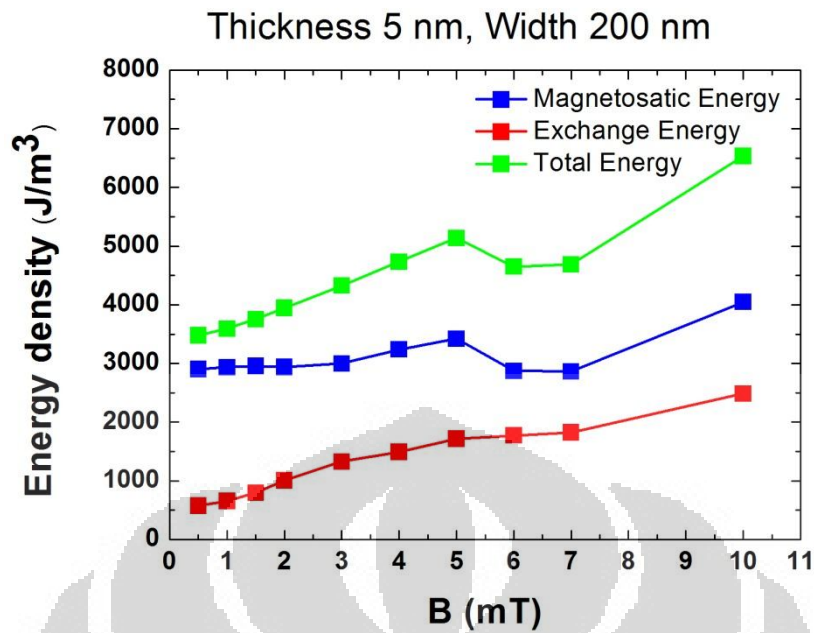
Figure 4.23 Magnetostatic and exchange energy density for simulated nanowire with thickness 5 nm and width 200 nm.

From this energy observation, it can be understood that the increase of exchange energy is needed for vortex/anti-vortex nucleation within nanowire. This means there is energy barrier for vortex/anti-vortex nucleation to overcome this energy barrier, there is must additional energy related to increases of exchange energy. Thus, in lower exchange energy, that is when external field doesn't exceed Walker Breakdown field, DW inner structure keeps transverse as long as propagating to the direction of external field. When the external field applied exceeds Walker Breakdown field, energy barrier is overcome and vortex/anti-vortex can be nucleated near the edge of the nanowire by pushing vortex/anti-vortex core cross the width of nanowire.

For further discussion about energy density in simulated nanowire, we plot total energy density against external field for various widths in figure 4.24 to figure 4.26.
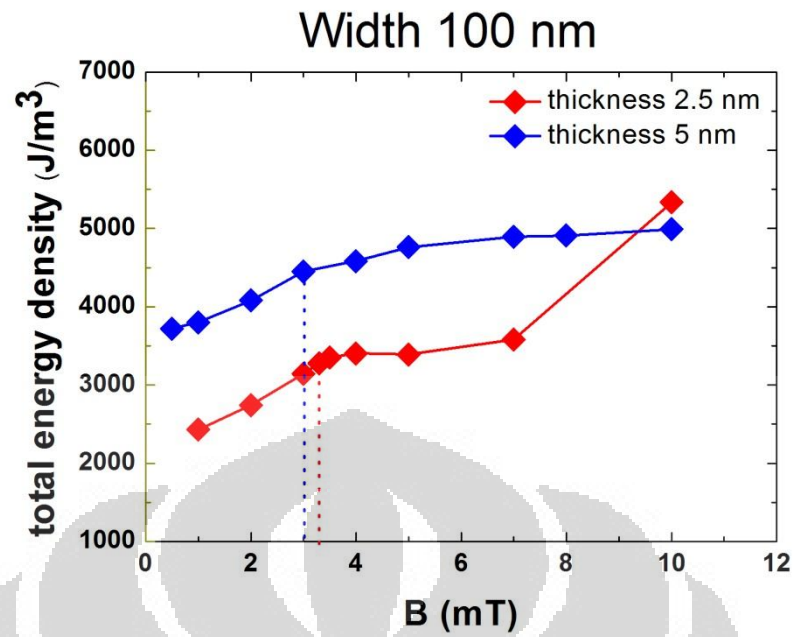
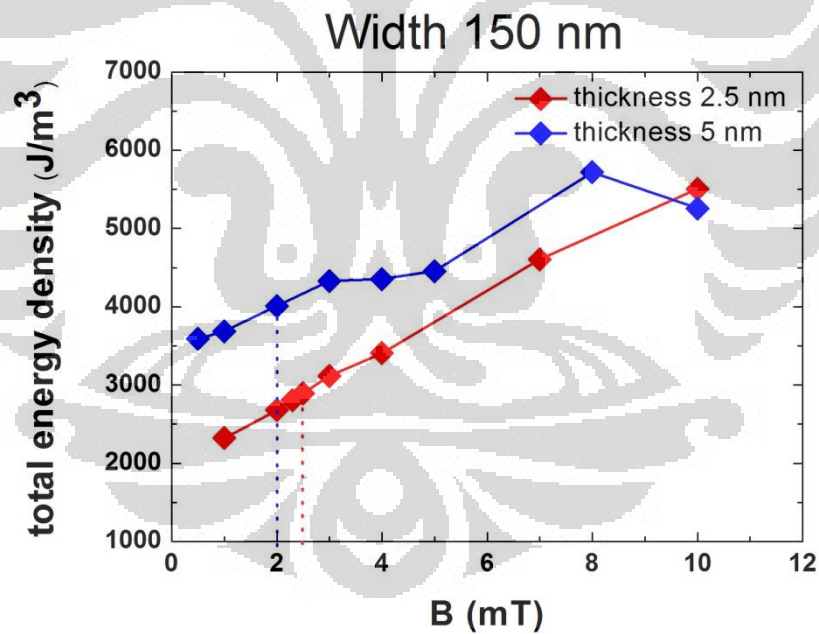Figure 4.24 Total energy density for simulated nanowire with width 100 nm.

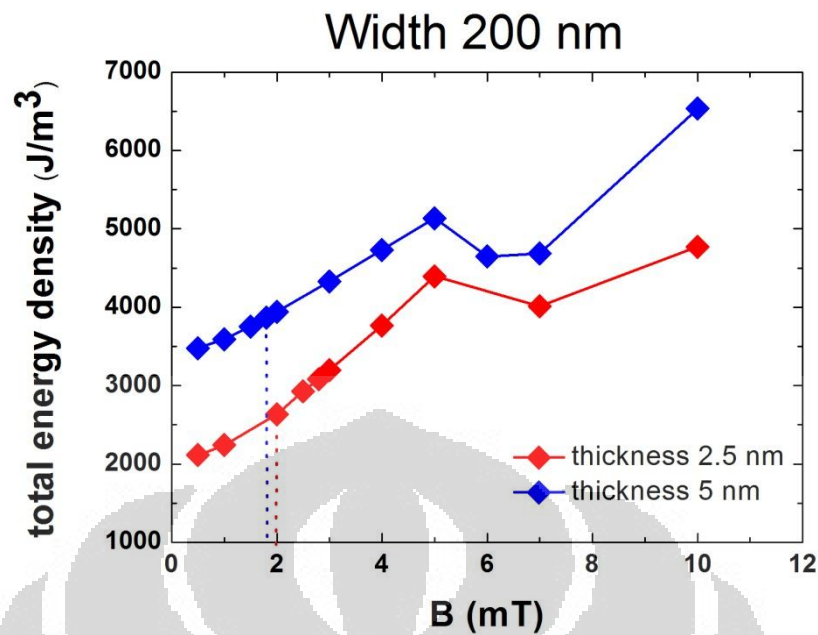Figure 4.25 Total energy density for simulated nanowire with width 150 nm.

Figure 4.26 Total energy density for simulated nanowire with width 200 nm.

Vertical dash line in all figures represents energy density in Walker Breakdown field. We can see for every width of nanowires, total energy density in thicker nanowire has higher value except in high field region. In high field region total energy density rise and then exceeding total energy density for thicker nanowire. We can observe this phenomenon for nanowire with width 100 nm and 150 nm.

Now we want to investigate magnetostatic energy density around Walker Breakdown field. Plot of magnetostatic energy density against external magnetic field was given in figure 4.27 to figure 4.29. It seems that nanowire dimension affect the characteristic of magnetostatic energy around Walker Breakdown field. Before Walker Breakdown, magnetostatic energy increase with external magnetic field where the magnitude of energy is greater for thicker nanowire. This characteristic confirm that, in small field the magnetostatic energy contribution in total energy is dominant than exchange energy.
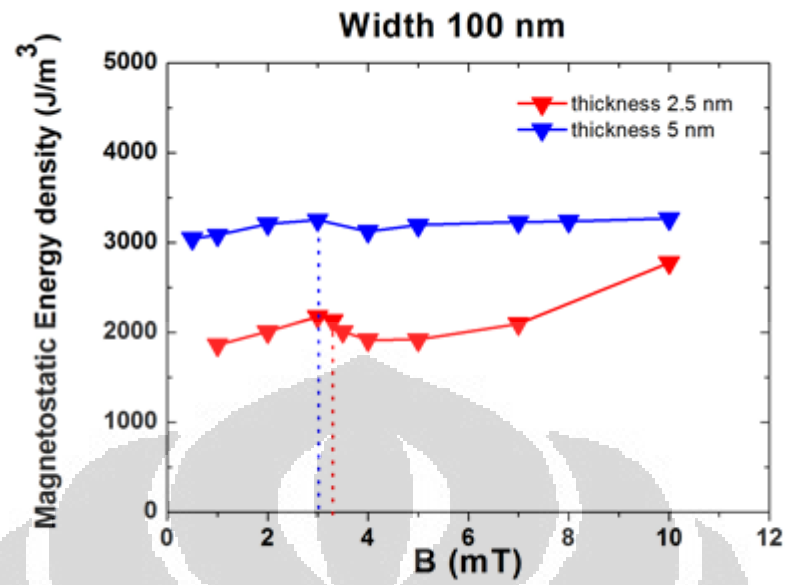
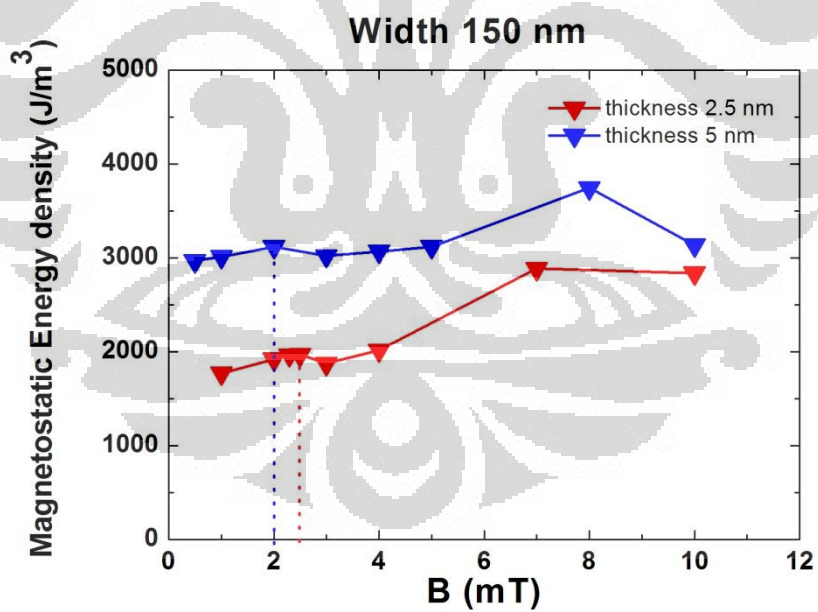Figure 4.27 Magnetostatic energy density for nanowire with width 100 nm.

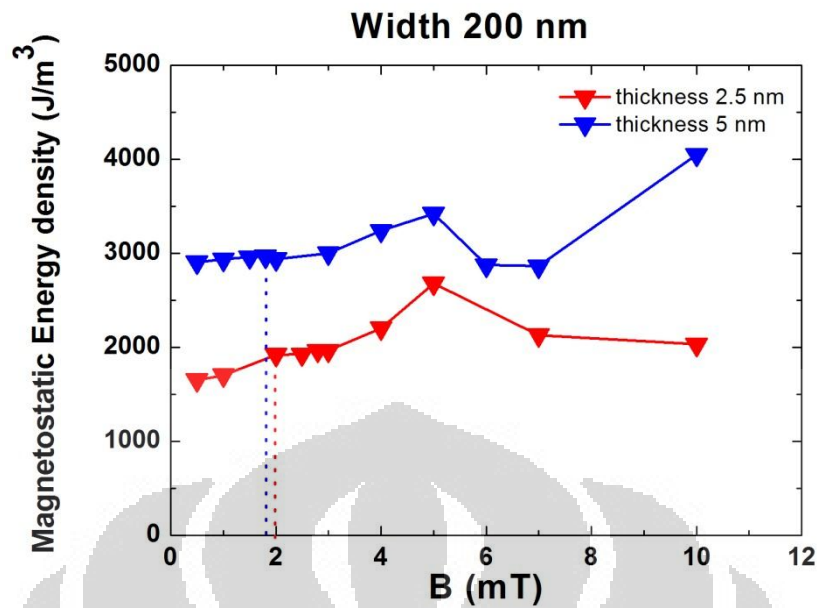Figure 4.28 Magnetostatic energy density for nanowire with width 150 nm.

Figure 4.29 Magnetostatic energy density for nanowire with width 200 nm.

For smallest dimension of nanowires, that is width 100 nm and thickness 2.5 nm; width 100 nm and thickness 5 nm; width 150 nm and thickness 2.5 nm; width 150 nm and thickness 5 nm, magnetostatic energy decrease as the external field increase. In thicker nanowire we can see that rate of change of magnetostatic energy is lower. Gradient of energy curve is steeper for nanowire with thickness 2.5 nm. When the dimension of nanowire is expanded (width 200 nm), magnetostatic energy didn't change too much and almost constant around Walker Breakdown field.

We also investigate exchange energy density around Walker Breakdown field. Figure 4.30 to figure 4.32 give a plot of exchange energy density curve. Exchange energy increase as the external magnetic field increase, for small field the magnitude of exchange energy is not differ in significant value for two thickness, but in high field region, the exchange energy is higher for nanowire for thickness 2.5 nm than thickness 5 nm. Around Walker Breakdown field, exchange energy increase more rapidly for a moment and increase again in high field region giving a high magnitude of exchange energy.
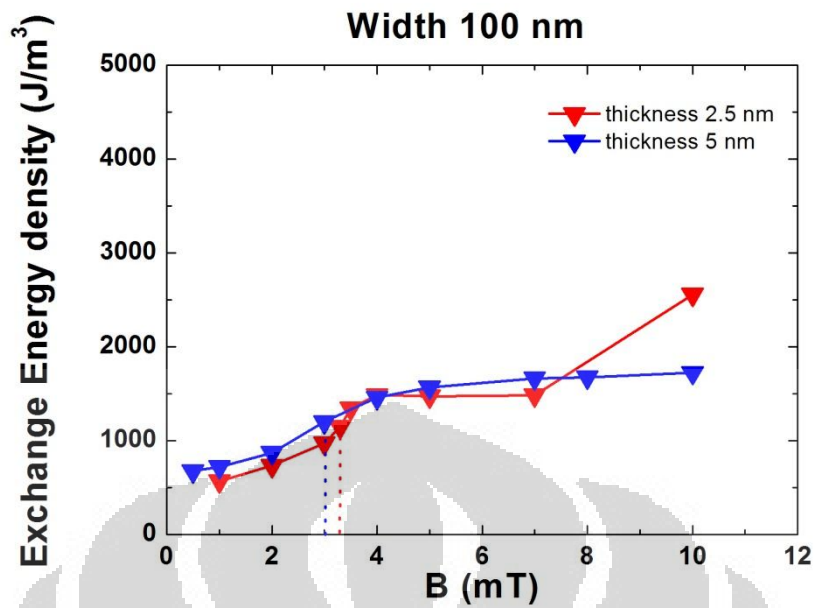
Figure 4.30 Exchange energy density for nanowire with width 100 nm.
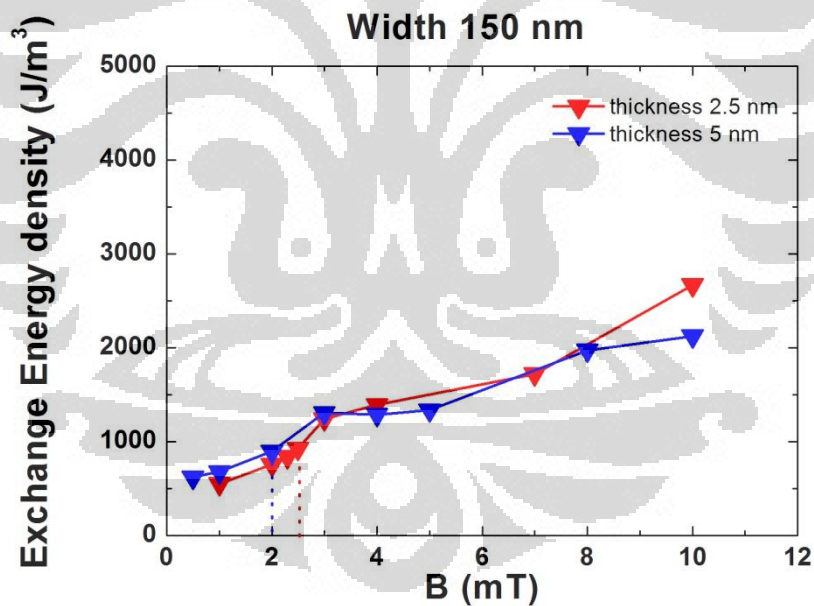

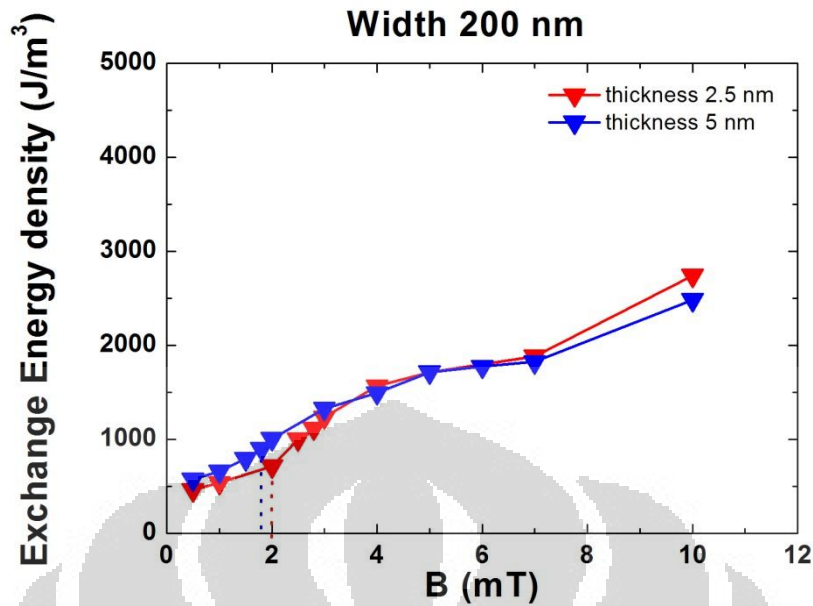Figure 4.31 Exchange energy density for nanowire with width 150 nm.

Figure 4.32 Exchange energy density for nanowire with width 200 nm.

Examine energy characteristic of nanowire in high field region is interesting. We observed that in low field region, exchange energy not differ in significant value for different width of the nanowire. However in high field region, exchange energy rising and have a greater value for wider nanowire. This can be observed in figure 4.33 for nanowire with thickness 2.5 nm and in figure 4.34 for nanowire with thickness 5 nm.

For magnetostatic energy term in different width of nanowires we observed similar behavior with exchange energy. Before Walker Breakdown this energy term is not differ too much within variation of width of nanowires. However, after Walker Breakdown field, this energy term have a tendency to rise as external field increase going to high field region. This characteristic give a significant different in magnetostatic energy for each nanowire with different width when we gave a higher external field. This plot of magnetostatic energy against external field is given in figure 4.35 and figure 4.36.
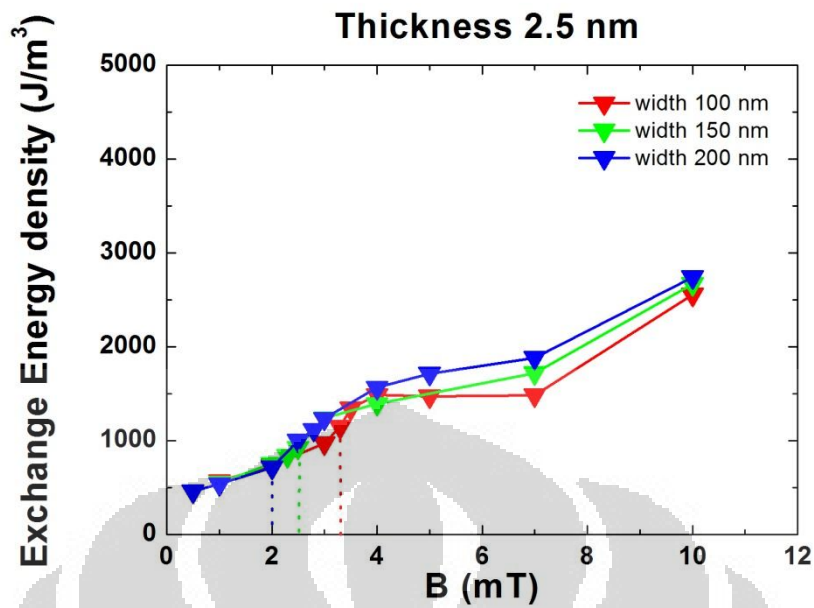
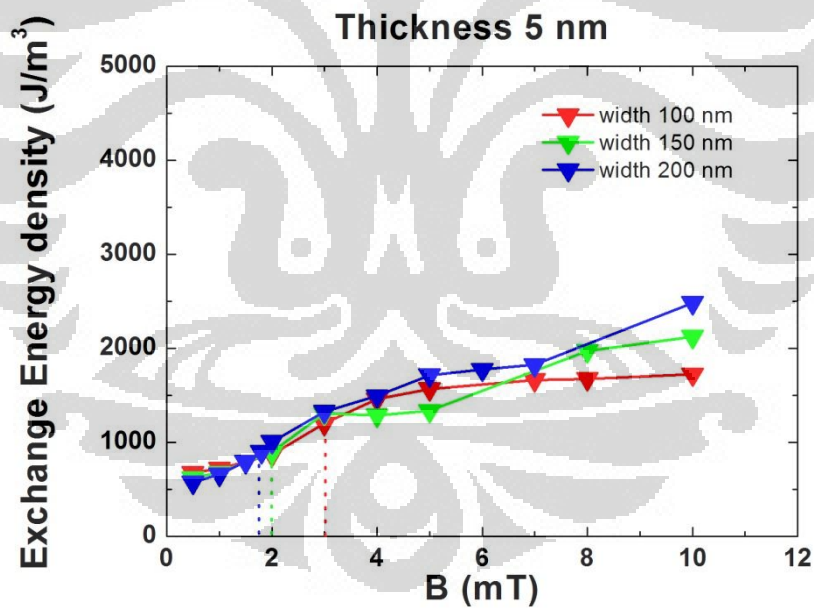Figure 4.33 Exchange energy density for nanowire with thickness 2.5 nm.

Figure 4.34 Exchange energy density for nanowire with thickness 5 nm.
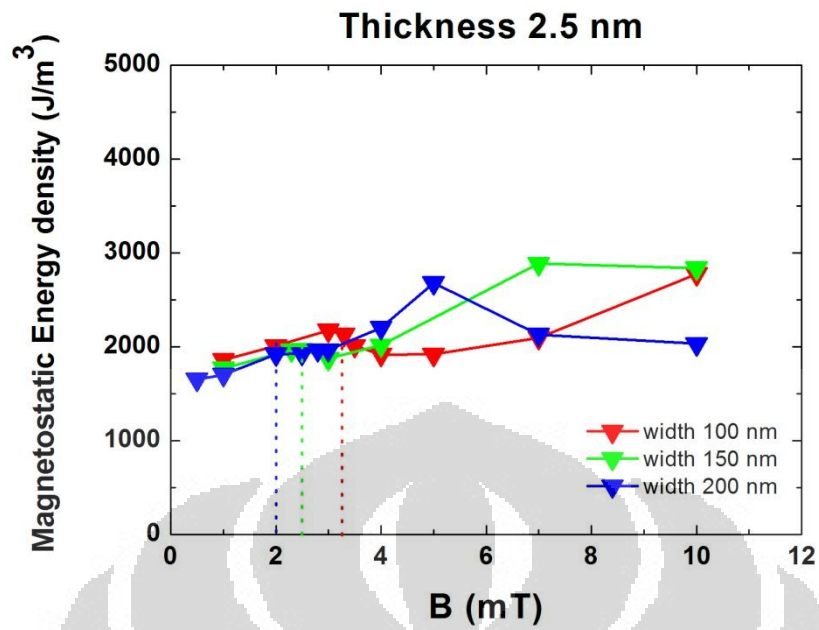
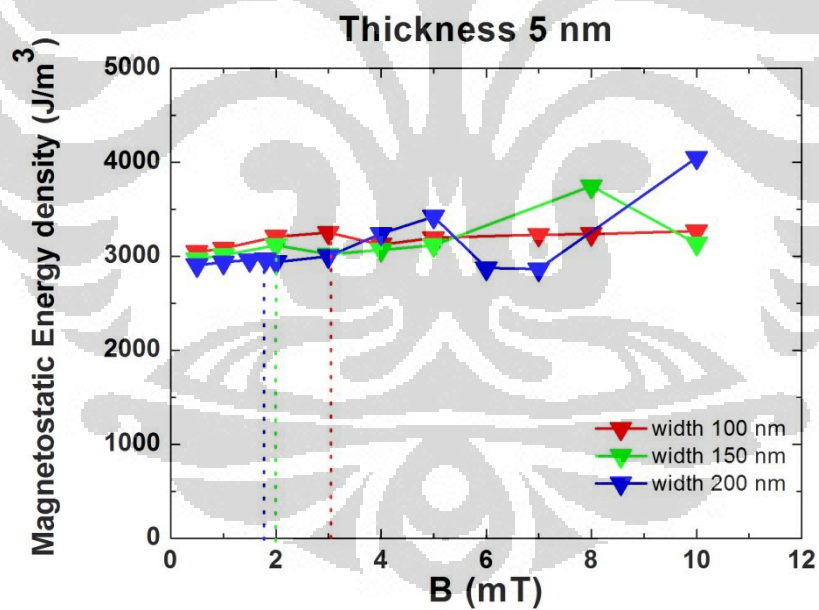Figure 4.35 Magnetostatic energy density for nanowire with thickness 2.5 nm.

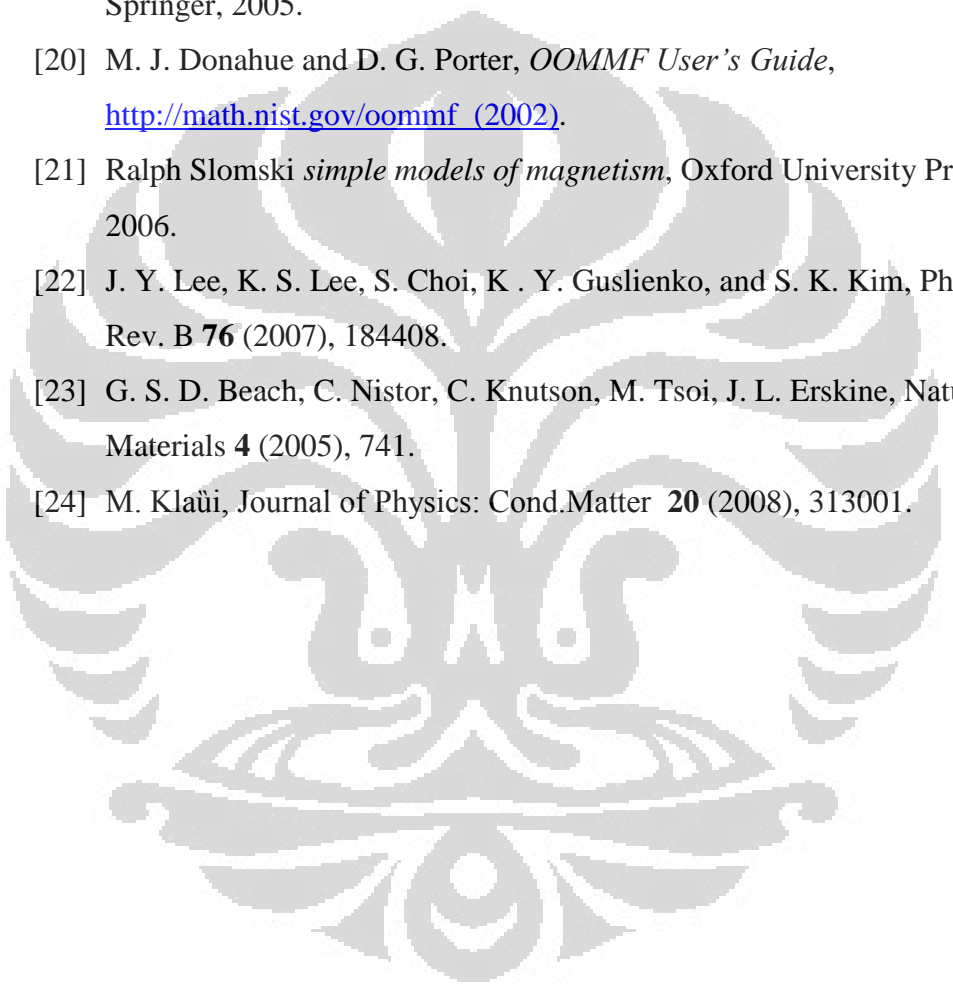Figure 4.36 Magnetostatic energy density for nanowire with thickness 5 nm.

Chapter 5
CONCLUSIONS

In conclusions, we have comprehensively investigated DW dynamics in ferromagnetic nanowires using micromagnetic simulations by means of public micromagnetic simulation software, OOMMF. We found that inner structure of DW is strongly dependent to nanowire geometry and external field applied and also influence average velocity of DW when propagate to the direction of external field. The main results of DW dynamic are as follows:

(a) The domain wall velocity increases as the external magnetic field increases and abruptly decrease after exceed Walker Breakdown field. The domain wall structure exhibits transverse domain wall before Walker breakdown field and keep transverse during propagate while vortex/anti-vortex domain wall appears after Walker breakdown field.

(b) Before reaching Walker breakdown field, DW velocity increase with increasing the width. This means at the wider nanowire, DW propagate with faster velocity. On the contrary, DW velocity decreases in the thicker nanowire.

(c) Walker breakdown field decrease with increasing the width and thickness of nanowires.

REFERENCES

[1]   M. N. Baibich, J. M. Broto, A. Fert, F. Nguyen Van Dau, and F. Petroff, Phys. Rev. Lett. **61**, 2472 (1988).

[2]   G. Binasch, P. Grunberg, F. Saurenbach, and W. Zinn, Phys. Rev B **39**, 4828 (1989).

[3]   M. Hayashi, L. Thomas, C. Rettner, R. Moriya, and S. S. P. Parkin, Nature Physics. **3**   (2007), 21.

[4]   S. A. Wolf, D. D. Awschalom, R. A. Buhrman, J. M. Daughton, S. von. Molnar, M. L. Roukes, A. Y. Chtchelkanova, and D. M. Treger, Science **294** (2001), 1488.

[5]   S. S. P, Parkin, M. Hayashi, and L. Thomas,Science **320** (2008), 190.

[6]   T. Ono, H. Miyajima, K. Shigeto, K. Mibu, N. Hosoito, T. Shinjo, Science **84** (1999), 68.

[7]   A. Thiaville, J. M. Garcia, and J. Miltat, J.Magn. Mag. Mat. **242** (2002), 1061.

[8]   R. D. Michael and M. J. Donahue, IEEE Trans. Magn. **33** (1997), 4167.

[9]   Y. Nakatani, A. Thiaville, and J. Miltat, J. Magn. Mag. Matter. **290** (2005), 750.

[10] J. Y. Lee, K. S. Lee, S. Choi, K. Y. Guslienko, and S. K. Kim, Phys. Rev. B **76** (2007), 184408.

[11] M. Klaui, J. Phys. Condens. Matter. **20** (2008), 313001.

[12] S. V. Tarasenko, A. Stankiewicz, V. V. Tarasenko, and J. Ferre, J. Magn. Magn. Matter **189** (1998),   19.

[13] D. Djuhana, H. G. Piao, S. H. Lee, D. H. Kim, S. M. Ahn andS. B. Choe, J. Appl. Phys. **97** (2010), 022511.

[14] D. Djuhana H. G. Piao, S. C. Yu, S. K. Oh, D. H. Kim, J Appl. Phys. **106**, 103926 (2009).

[15] T. L. Gilbert, IEEE Trans.Magnetics. **40** (2004), 3443.

[16] B. Hillebrands and K. Ounadjela, *Spin Dynamics in Confined Magnetic Structure II*, Springer-Verlag Berlin Heidelberg, 2003.

[17] Matiaz getzlaf, *Fundamentasl of Magnetism*, Springer-Verlag Berlin Heidelberg, 2007.

[18] C. Kittel, *Introduction to Solid state physics 8th*, John Wiley & sons, Inc, 2005.

[19] J. D. Patterson, B. C. Bailey, *Solid State Physics introduction to theory*, Springer, 2005.

[20] M. J. Donahue and D. G. Porter, *OOMMF User's Guide*, http://math.nist.gov/oommf (2002).

[21] Ralph Slomski *simple models of magnetism*, Oxford University Press, 2006.

[22] J. Y. Lee, K. S. Lee, S. Choi, K . Y. Guslienko, and S. K. Kim, Phys. Rev. B **76** (2007), 184408.

[23] G. S. D. Beach, C. Nistor, C. Knutson, M. Tsoi, J. L. Erskine, Nature Materials **4** (2005), 741.

[24] M. Klaüi, Journal of Physics: Cond.Matter **20** (2008), 313001.